eNeuro

Research Article: New Research | Disorders of the Nervous System

RIGHT STRUCTURAL AND FUNCTIONAL REORGANIZATION IN 4-YEAR-OLD CHILDREN WITH PERINATAL ARTERIAL ISCHEMIC STROKE PREDICT LANGUAGE PRODUCTION

https://doi.org/10.1523/ENEURO.0447-18.2019

Cite as: eNeuro 2019; 10.1523/ENEURO.0447-18.2019

Received: 12 November 2018
Revised: 24 April 2019
Accepted: 3 June 2019

RIGHT STRUCTURAL AND FUNCTIONAL REORGANIZATION IN 4-YEAR-OLD CHILDREN WITH PERINATAL ARTERIAL ISCHEMIC STROKE PREDICT LANGUAGE PRODUCTION

Abbreviated title: Brain plasticity mechanisms after perinatal stroke

Clément François[1,2†], Pablo Ripollés[3†], Laura Ferreri[1,2], Jordi Muchart[4], Joanna Sierpowska[1,2], Carme Fons[4], Jorgina Solé[2], Monica Rebollo[4], Robert J Zatorre[8], Alfredo Garcia-Alix[4,7], Laura Bosch[2,10*] & Antoni Rodriguez-Fornells[1,2,11*]

[1]Cognition and Brain Plasticity Group [Bellvitge Biomedical Research Institute-] IDIBELL, L'Hospitalet de Llobregat, 08907, Barcelona, Spain.

[2]Department of Cognition, Development and Educational Science, University of Barcelona, 08035, Barcelona, Spain.

[3]Poeppel Lab, Department of Psychology, New York University, 10003, New York, USA.

[4]Institut de Recerca Sant Joan de Déu. Hospital Sant Joan de Déu, Universitat de Barcelona, 08950, Barcelona, Spain.

[5]Radboud University, Donders Institute for Brain, Cognition and Behaviour, Nijmegen, The Netherlands.

[6]Radboud University Medical Center, Department of Medical Psychology, Nijmegen, The Netherlands.

[7]Pediatric Neurology Department. Hospital Sant Joan de Déu. Institut de Recerca Pediàtrica. Hospital Sant Joan de Déu, Universitat de Barcelona, 08950, Barcelona.

[8]Cognitive Neuroscience Unit, Montreal Neurological Institute, McGill University, H3A 2B4, Montreal, Canada.

[9]CIBER de Enfermedades Raras (CIBERER). U724, Madrid, Spain.

[10]Institute of Neuroscience (UBNeuro), University of Barcelona, 08035, Barcelona, Spain.

[11]Catalan Institution for Research and Advanced Studies, ICREA, 08010, Barcelona, Spain.

†: co-first authorship.

Author contributions

CFr, PR, LB, AGA, RJZ, and ARF Designed Research; AGA, CFo, JM and MR provided access to the patients; CFr, PR, JSo and LB Performed Research; CFr, PR, LF, and JSi Analyzed Data; CFr, PR, LB and ARF Wrote the paper.

***Correspondence should be addressed to**

Antoni Rodriguez-Fornells, Department of Cognition, Development and Educational Science, University of Barcelona, Campus de Bellvitge - Pavelló de Govern, 08908 L'Hospitalet de Llobregat (Barcelona - Spain). Email: antoni.rodriguez@icrea.cat

Laura Bosch, Department of Cognition, Development and Educational Science, University of Barcelona, Barcelona, Spain. Email: laurabosch@ub.edu

Number of figures: 7
Number of tables: 4
Number of Multimedia: 0
Number of words for abstract: 225
Number of words for Introduction: 704
Number of words for Discussion: 1763

Acknowledgements: We wish to thank all the children and their families for their enthusiasm in participating in the present study. We also thank Dr. Helena Gaïtan for her help during the collection of the data as well as Dr. John E. Richards for giving us access to the Neurodevelopmental MRI Database. (http://jerlab.psych.sc.edu/NeurodevelopmentalMRIDatabase/).

This work was partially funded by the "Plan Nacional de I+D+I and ISCIII-Subdirección General de Evaluación y Fomento de la Investigación Sanitaria", Project PI15/00846, the European Regional Development Fund (FEDER “a Way to Build Europe”), a SLT002/16/00390 grant, funded by the Department of Health of the Generalitat de Catalunya by the call “Acció instrumental d'incorporació de científics i tecnòlegs” to CFr, a grant from the Bial Foundation to ARF and a Spanish MINECO project (PSI 2014-55105P) to LB.

Conflict of interests: The authors declare that they have no conflict interests

Abstract

Brain imaging methods have contributed to shed light on the mechanisms of recovery after early brain insult. The assumption that the unaffected right hemisphere can take over language functions after left perinatal stroke is still under debate. Here, we report how patterns of brain structural and functional reorganization were associated with language outcomes in a group of 4-year-old children with left perinatal arterial ischemic stroke. Specifically, we gathered specific fine-grained developmental measures of receptive and productive aspects of language as well as standardized measures of cognitive development. We also collected structural neuroimaging data as well as functional activations during a passive listening story-telling fMRI task and a resting state session (rs-fMRI). Children with a left perinatal stroke showed larger lateralization indices of both structural and functional connectivity of the dorsal language pathway towards the right hemisphere that, in turn, were associated with better language outcomes. Importantly, the pattern of structural asymmetry was significantly more right-lateralized in children with a left perinatal brain insult than in a group of matched healthy controls. These results strongly suggest that early lesions of the left dorsal pathway and the associated perisylvian regions can induce the inter-hemispheric transfer of language functions to right homolog regions. This study provides combined evidence of structural and functional brain reorganization of language networks after early stroke with strong implications for neurobiological models of language development.

Significance statement

The prevalent theories explaining the functional recovery of language functions after perinatal ischemic stroke strikingly differ on the role of perilesional functionally spared regions as opposed to the homologous non-affected contralesional brain areas. Here, we assessed how patterns of brain functional and structural reorganization were associated with language outcomes in a group of 4-year-old children with left perinatal arterial ischemic stroke. Larger lateralization indices of both functional and structural connectivity towards the right hemisphere were associated with higher levels of language development. Thus, inter-hemispheric plasticity through structural and functional hyper-connectivity mechanisms might be crucial in early damage, probably through the degeneration of neurons projecting from temporal to frontal areas together with contralateral axonal sprouting over the right hemisphere.

Introduction

In adults, language processing relies on a largely distributed network mainly involving perisylvian brain regions in the left hemisphere (Friederici 2011; Price, 2012). These brain areas are interconnected through white matter fiber bundles, altogether forming the dorsal and ventral pathways involved in language processing (Catani et al., 2005; Hickok & Poeppel, 2007; Rauschecker & Scott, 2009). According to the dual-stream models, the dorsal pathway includes the arcuate fasciculus (AF) composed of the long segment that connects superior posterior temporal regions with Broca's area, the anterior segment connecting the inferior parietal lobe (IPL) with Broca's area, and the posterior segment from pST regions to the IPL (Catani et al., 2005; 2007). Functionally, the AF is known to contribute to sound-to-articulation transformations (Hickok & Poeppel, 2007; Liberman & Mattingly, 1985), phonological word-learning (Lopez-Barroso et al., 2013), audio-motor integration (Assaneo et al., 2019), phonological processing (Vandermosten et al., 2012) and working memory (Meyer et al., 2014). The ventral stream connects the occipital superior temporal, angular gyrus and inferior frontal gyri and is formed by the inferior fronto-occipital (IFOF), inferior longitudinal (ILF) and uncinate fasciculi (UF) (Bajada, Lambon Ralph, & Cloutman, 2015). This ventral pathway rather contributes to semantic processing, sound-to-meaning mapping, semantic word-learning and auditory object recognition (Catani et al., 2003; Friederici, 2009; Saur et al., 2008; Ripolles et al., 2017). Interestingly, neuroimaging studies have revealed that newborns may recruit a bilateral neural network with an already left predominance for linguistic stimuli (Dehaene-Lambertz & Spelke, 2015; Shultz et al., 2014). Although it is still under debate, some of the white-matter tracts such as the AFare already developed and functional at birth, while others such as the UF are still developing due to a delayed maturation (Brauer et al., 2013; Bajada, Lambon Ralph, & Cloutman, 2015; Perani et al., 2011; Zhang et al., 2007). Despite the fact that low-level language functions may already be present at birth, as reflected by left cortical activations for specific spectro-temporal features of the speech input (Dehaene-Lambertz et al., 2002, 2006; Perani et al., 2010; Telkemeyer et al., 2009), the later development of higher-order language functions may involve a graded lateralization toward the left hemisphere emerging with age (Brown et al., 2005; Szaflarski et al., 2006). For instance, the cortical maturation of temporoparietal regions has been shown to occur much slower than the maturation of frontal brain regions (Leroy et al., 2011). This slow maturation has also been evidenced at the white matter level with a slower maturation and higher sensitivity to environmental factors of the right posterior segment of the arcuate fasciculus (AF) as compared to the anterior and long segments (Budisavljevic et al., 2015). These results favor a plastic and experience-dependent view of the neural bases of language acquisition in typically developing children.

In this context, the study of young children with early brain lesions such as perinatal arterial ischemic stroke (PAIS) provide a unique opportunity to study brain reorganization and plasticity mechanisms taking place before language development unfolds. PAIS occurs in one in 4000 births (Nelson & Lynch, 2004) and may have long-term negative effects on children's cognitive development and language functions compared to typically developing peers (Ballantyne et al., 2008; Reilly, et al., 2013; Westmacott et al., 2009). Nonetheless, as opposed to stroke occurring during adulthood, PAIS over the left hemisphere does not generally induce post-stroke aphasia (Bates et al., 2001; Stiles et al., 2005) even though very recent data suggest the possible existence of a developmental form of conduction aphasia after neonatal stroke (Northam et al., 2018; Schlaug, 2018). Due to the low incidence of PAIS, no previous neuroimaging studies have been conducted in this population during the pre-school period when learning and neuroplastic processes are taking place. Here, we assessed for the first time how patterns of brain structural and functional reorganization were associated with language outcomes in a group of 4-year-old children with left PAIS. To this aim, we gathered fine-grained measures of receptive and productive aspects of language as well as standardized measures of cognitive development. We also collected both structural and functional neuroimaging data under light anesthesia. Importantly, we used a group of healthy children from the Pediatric MRI Data Repository (NIH MRI Study of Normal Brain Development) matched in age and gender to serve as a control for the structural connectivity analyses.

Considering the role of perilesional functionally spared regions as opposed to the homologous non-affected contralesional brain areas in the current theories of functional recovery after early stroke, we expected children with perinatal stroke affecting the left AF to be the most impaired in language functions. This pattern of results would confirm that the functional integrity of the left hemisphere is mandatory to achieve normal language development (Raja-Beharelle et al., 2010). However, if the right hemisphere is able to "take over" language functions usually supported by the left hemisphere (Staudt et al., 2002; Tillema, et al., 2008; Tivarus et al., 2012), then we should observe a significant relationship between structural parameters (i.e., microstructural properties of language-related white matter pathways) and/or functional activations in the right hemisphere and measures of receptive and expressive language, in line with previous evidence from adults on the role of the right dorsal pathway in recovery from left stroke-induced aphasia (Forkel et al., 2014; Pani et al., 2016).

Material and Methods

Ethics and Participants

Six children with symptomatic perinatal arterial ischemic stroke (2 girls) over the left hemisphere took part in the present study. These children were part of a larger prospective observational multicenter study about acute symptomatic perinatal arterial ischemic stroke (PAIS). The selection of these children was made based on the minimum age at which the behavioural and neuroimaging evaluations could be done at a reasonable time interval for all of them. All but 2 children received speech therapy on a weekly basis (L2 and L6). Symptomatic PAIS was defined as the finding of an ischemic lesion by magnetic resonance imaging (MRI) study in the territory of the main cerebral arteries (middle cerebral artery [MCA], anterior cerebral artery [ACA], and posterior cerebral artery [PCA]) in an infant presenting with seizures, recurrent apnea or acute neurological deficit during the first days of life. Infants with (i) clear sign of tissue loss or atrophy in MRI suggestive of an old infarction that occurred before birth; (ii) vascular malformation; (iii) congenital or chromosomic anomalies; (iv) metabolic or infectious diseases; (v) complex heart congenital diseases or infants with Extra Corporeal Membrane Oxygenation, were excluded from the study. Specifically, MRI-based diagnostics were performed on anatomical data acquired on a 1.5 T whole-body MRI scanner with a specific neonatal head coil within 7 days after the occurrence of the neurologic symptoms. These MRI data allowed classifying the lesions according to the arterial territory involved (i.e. four segments: M1-M4). The classification of each infarct was obtained by two independent neurologists blind to the clinical data. Discrepancies in the classification of the PAIS were discussed and solved by consensus at joint revaluation among three observers: AGA and two neurologists blind to the clinical data. Motor impairment was considered when infants had clear clinical signs of monoplegia/ hemiplegia (GMFCS at least I and/or BFMF at I level). Infants with minor abnormalities such as precocious handedness, mild abnormalities of tone or reflexes that did not interfere with functions were not considered to have a motor impairment. Importantly, while all children presented with seizures during the 3 first days following birth, no children suffered from epilepsy at the time of the MRI scan

Brain MRI was also acquired at 3.8 years (SD = 0.26) to control for the residual lesion and to obtain the functional and structural data reported here. These MRI data demonstrated that all children had infarctions of the middle cerebral artery affecting several brain regions (see **Table 1** and **Figure 1**). At the time of the study, all the children showed a right-hand preference. The parents of the children received information on the study in written and spoken form and their written consent was obtained before the study begun. The study was approved by the Ethics Committee of a location which will be identified if the article is published in accordance with the Declaration of Helsinki.

In addition, we used a group of 9 healthy children (3 females, 4.30 ± 1.09 years of age) from an MRI pediatric repository to serve as a control for the structural connectivity analyses.

The control group and the patients were matched in age [t (13) = 1.02; P = .32. No difference in gender was found (X^2 = 0.313; P = .57). In particular, data used in the preparation of this article were obtained from the Pediatric MRI Data Repository created by the NIH MRI Study of Normal Brain Development (we searched for all children data between 3 and 6 years old having DW-MRI data). This is a multi-site, longitudinal study of typically developing children, from ages newborn through young adulthood, conducted by the Brain Development Cooperative Group and supported by the National Institute of Child Health and Human Development, the National Institute on Drug Abuse, the National Institute of Mental Health, and the National Institute of Neurological Disorders and Stroke (Contract #s N01-HD02-3343, N01-MH9-0002, and N01-NS-9-2314, -2315, -2316, -2317, -2319 and -2320). A listing of the participating sites and a complete listing of the study investigators can be found at http://www.bic.mni.mcgill.ca/nihpd/info/participating_centers.html. This manuscript reflects the views of the authors and may not reflect the opinions or views of the NIH.

Neuropsychological assessment

Standard neuropsychological testing

Cognitive functions in the domains of memory and learning, visuospatial processing, sensorimotor skills, and language were assessed using the NEPSY-II battery with the specific subtest suitable to test 3- to 4-year-old children (Korkman et al., 2007, Spanish adaptation). Specifically, we assessed: a) language functions (subtests: comprehension of instructions; body part naming and identification; words generation; phonological processing; and speeded naming); b) memory and learning functions (subtests: memory for designs; narrative memory; and sentence repetition); c) visuospatial processing (subtests: block construction; and design copying); and d) sensorimotor processing (subtests: imitating hand positions and, visuomotor precision). Raw scores for each sub-test were converted into scalar values and compared to normative values (mean=10, SD=2).

Language measures

Receptive vocabulary was assessed using the Peabody Picture Vocabulary Test (PPVT-III, Dunn et al., 1997, with Spanish norms) which offers a raw score that can be transformed into a percentile rank, a receptive verbal IQ (mean=100, SD=15) and the corresponding developmental age.

Phonological development assessed phonological production of 32 common words, mostly disyllabic, involving 15 different word shapes and covering all consonantal segments and segment combinations in Spanish (Bosch, 2004). This assessment tool uses pictures favoring utterance production rather than simple naming. From children's spontaneous

production, phonological mean length of utterance (pMLU, i.e. phonological complexity based on the accuracy in producing consonants, diphthongs, and complex syllabic structure) and phonological whole-word proximity to the corresponding adult word-form (i.e. proximity) scores were obtained for complexity and closeness to the target productions respectively (Ingram 2002). The pMLU of the word list from this tool is 8.31. This would be the value obtained if all target words were correctly produced, the Proximity score in this case (child's pMLU/target pMLU) being 1. Analysis of the original data from a sample (N = 50) of 4-year-old children from Bosch (2004), used as a reference group, yielded the following values: mean pMLU = 7.55 (SD = 0.55) and mean Proximity score =0.91 (SD = 0.064).

Expressive language complexity was assessed from recordings of spontaneous utterances produced in a semi-structured conversation/play situation using toys and picture books. The children's spontaneous utterances were transcribed so that the values of the mean length of utterance in words (MLU) and the MLU of the five longest utterances (max-L) could be obtained. These measures could then be compared to the reference values from an age-matched control group of N = 50 Spanish-speaking children at age 4 years (Fernández & Aguado, 2007). Mean MLU in words for this reference group is 3.91 (+/- 1 SD: 4.45 – 3.37). Mean value of the max-L score is 10.56 (+/- 1 SD: 12.47 – 8.65).

Statistical analysis

At the individual level, the data from each patient were compared with the level of performance of an age-matched control group. The comparisons were performed using the modified *t*-test, which is specifically designed to compare an individual to a small sample of control participants (Crawford, Garthwaite, & Porter, 2010).

At the group level, Mann-Whitney tests for independent samples were used to compare the behavioral scores of children with stroke to those of a control group when present (i.e. phonological measures of complexity and proximity–pMLU–and utterance complexity in spontaneous speech–MLU and L-max).

MRI procedure

Sedation procedure.

We followed exactly the same procedure as in a previous paper (François et al., 2016). Specifically, in order to reduce movement artifact of the participant during the MRI examination, the children were previously sedated as recommended in pediatric functional neuroimaging (Lai et al., 2011; DiFrancesco et al., 2013; Souweidane et al., 1999; Bernal et al., 2012; Kerssens et al., 2005). The children were evaluated by the anesthesiologist and food

intake restriction was controlled. First, and with the aim of acquiring structural MRI information (structural MRI and DW-MRI sequences require precise and careful control of infant's head and body movements), anesthesia was induced via a mask with sevoflurane which is the routine method used in François and colleagues (2016). Immediately after this procedure, the intravenous line was placed, and the children were transitioned to an intravenous-based anesthetic with propofol. The initial propofol dose was adjusted to render the children motionless but able to maintain his or her airway with a laryngeal mask**.** Propofol dosage for induction was 2 mg/kg and after perfusion, a dosage of 8-10 mg/kg/hour was administered. The dosage was decreased to 6 mg/kg/hour until the end of the procedure. Both sevoflurane and propofol have very small side effects and are drugs routinely used in pediatric neuroimaging. Duration of sedation using both drugs is very small, allowing for very fast recovery times (Bernal et al., 2012). Importantly, we considered the pharmacokinetics of sevoflurane in order to ensure that functional tasks were carried exclusively under propofol anesthesia. Because of this, we induced a fast transition to propofol anesthesia after sevoflurane and also, we ran the first eighteen minutes of the structural imaging part ensuring that the possible effect of sevoflurane in the subsequent fMRI task was minimum. Indeed, the low solubility of sevoflurane in the blood induces a rapidly decreasing alveolar concentration after cessation of the inhaled agent which is linked to very fast recovery times and wash out (Yasuda et al., 1991; Bernal et al., 2012). However, and given that propofol can reduce connectivity in cortical areas of significance for the current study (Boveroux et al., 2010), we reconstructed standard resting-state fMRI networks (i.e., the Default-Mode Network) using Independent Component Analysis (ICA) as a demonstration of data quality. Pre-processed resting state data from all patients (see below *fMRI preprocessing and statistical analyses;* data were normalized to a 4-year-old template space) were submitted to Group Spatial ICA, using the Group ICA of fMRI Toolbox (GIFT v4.0b; http://mialab.mrn.org/software/gift/; Calhoun et al., 2001a). The mean value per time point was removed and data were concatenated and reduced to 10 independent components using a two-step principal component analysis and the infomax algorithm (Bell and Sejnowski, 1995). Finally, data were scaled to Z-scores. To obtain whole brain group-wise statistics, the spatial map of each of the ICA components (i.e., networks) retrieved for all participants was submitted to a second-level analysis using a one sample t-test under SPM12, which treats each subject's spatial map as a random effect (Calhoun et al., 2001b). The Default Mode Network (DMN) was selected by visually inspecting this group results. This group DMN along with each patient´s individual DMN are shown in Fig. 1B.

MRI scanning.

MRI data were collected on a 1.5 T whole-body MRI scanner at a location which will be identified if the article is published (GE Signa HD). The acquisition of a high-resolution T1-w structural image (magnetization-prepared rapid acquisition gradient echo sequence; TR=12.396 ms, TE=5.22 ms, slice thickness=0.4297 mm, 1 mm in-plane resolution, 180 slices, matrix size=512x512) was followed by a DW-MRI sequence. DW-MRI scans were acquired with a spin-echo echo-planar imaging (EPI) sequence (TR=16500 ms, TE=100 ms, 48 axial slices, slice thickness 2.5 mm, FOV: 270, acquisition matrix: 100 ×100, reconstruction matrix: 256 × 256, voxel size: 1.05× 1.05× 2.5 mm^3). One run with one non-diffusion weighted volume (using a spin-echo EPI sequence coverage of the whole head) and 29 diffusion-weighted volumes (b-value of 1500 s/mm^2) was acquired. One final FLAIR image (TR=11002 ms, TE=95 ms, slice thickness=0.3711 mm, 4.5 mm in-plane resolution, 35 coronal slices, matrix size=512x512) was also collected. After structural data was collected, a fMRI language task was carried out. One functional run consisting of 120 (6 minutes) functional images sensitive to blood oxygenation level-dependent contrast (BOLD; echo planar T2*-weighted gradient echo sequence; TR=3000 ms-as in Perani et al., 2010; 2011-, TE=60 ms, flip angle 80°, acquisition matrix =64×64, 3.75 mm in-plane resolution, 3.5 mm thickness, no gap, 34 axial slices aligned to the plane intersecting the anterior and posterior commissures) was acquired. Additionally, 100 volumes (5 minutes) of resting state (no stimuli were presented during acquisition) were collected using the same acquisition parameters as for the passive listening task.

DW-MRI data for the control group were part of the Expanded Diffusion Tensor Imaging Release 5.1 of the NIH Pediatric MRI Data Repository (5 controls: Siemens, 10 volumes with b=0 s/mm^2 and 50 directions with a b-value of 1100 s/mm^2, TR: 7900 ms, TE: 87 ms, 60 axial slices, FOV: 240, acquisition matrix: 96 × 96, voxel size: 2.5× 2.5× 2.5 mm^3; 1 control with same parameters as the previous, but with 7 b0s and 46 directions; 1 control with same parameters as the first 5 controls, but with TR: 7800ms and TE:85; 1 control with same parameters as the first 5 controls, but with TR: 8700ms and 66 axial slices; 1 control, General Electric, Siemens, 2 volumes with b=0 s/mm^2 and 15 directions with a b-value of 1100 s/mm^2, TR: 19580.5 ms, TE: 84.8 ms, 60 axial slices, FOV: 240, acquisition matrix: 9 × 96, voxel size: 1.88 × 1.88 × 2.5 mm^3).

fMRI experimental design

For the language task, we used a spontaneous narration of a short children story (The Snowman by Raymond Briggs) recorded in child-directed speech by a female native Spanish speaker. The story was divided into ten blocks of 20 seconds, each block containing short sentences forming a sequence of complete intonation phrases.

As an acoustic control for the language task, we generated music-like stimuli composed of sequences of discrete tones using the technique developed in Patel and colleagues (1998 see also Liu et al., 2010) for converting intonation patterns of spoken utterances to tone analogs. For each language sentence, a tone sequence was synthesized with the same pitch and temporal patterns as for the sentence's syllables. First, discrete tone analogs were generated for each syllable in every sentence using a specific algorithm. This new sound represented the sum of the fundamental frequency at the median F0 of the original syllable [= (max F0 + min F0)/2] plus its seven odd harmonics (of the same amplitude and with sine phase) and was sampled at 44.1 KHz. Importantly, the tone analog had the same duration as the original syllable, in order to equate syllable duration. An 8 ms onset and offset taper was later applied to the tone to adjust the rise/decay time. The tone analogs of all the syllables and in each sentence were combined together, preserving the silent gaps as in the originally spoken utterances, to form a discrete-tone sequence. Using this technique we ensured that each speech sentence had a musical-phrase correspondence comparable in overall parameters such as length, rate as well as in more fine-grained patterns of frequency and timing.

Ten blocks of 20 seconds containing the original story (Language condition) or its musical analog (Control condition) were presented in order, with 15 seconds rest periods between blocks where no stimuli were presented (Rest condition). The off-resting periods were set to 15 s because the BOLD response in children returns to baseline levels faster than in adults (see Richter & Richter, 2012; Blasi et al., 2011).

fMRI preprocessing and statistical analysis

Data were pre-processed using Statistical Parameter Mapping software (SPM8, Wellcome Trust Centre for Neuroimaging, University College, London, UK, www.fil.ion.ucl.ac.uk/spm/). The functional images (language task and the rs-fMRI data) was first realigned, and then co-registered to the corresponding T1 using FSL's FLIRT (FMRIB's Linear Image Registration Tool; Jenkinson et al., 2012). As stated before, we used an age-appropriate template to register the children MRI images to the same space (Richards et al., 2015). In particular, we employed FSL's FNIRT (FMRIB's Nonlinear Image Registration Tool; Jenkinson et al., 2012), to normalize our patient's T1-w and its corresponding lesion mask to a 4 year-old MRI brain template obtained from the Neurodevelopmental MRI Database (http://jerlab.psych.sc.edu/NeurodevelopmentalMRIDatabase/access.html; Almli et al., 2007; Sanchez et al., 2011; Richards et al., 2015; Fillmore et al., 2015). We first linearly registered the individuals' T1-w and the corresponding lesion map to the 4-year old template using FLIRT. Then, we used FNIRT to non-linearly register the children T1 images to the aforementioned

age-specific brain template. For all these steps, cost function masking was employed (Brett et al., 2001; Andersen et al., 2010; Ripolles et al., 2012). The registration parameters obtained during these calculations were applied to the lesion masks, the fMRI and the rs-fMRI data (previously registered to the corresponding T1) to normalize it to the common space (the 4-year-old template). Finally, fMRI and rs-fMRI data were spatially smoothed with an 8 mm FWHM kernel.

Finally, an fMRI group analysis was performed. First, a blocked-design matrix was specified using the canonical hemodynamic response function. Three different conditions were specified: Language, Control, and Rest. Data were high-pass filtered (to a maximum of 1/128Hz) and serial autocorrelations were estimated using an autoregressive (AR(1)) model. Remaining motion effects were minimized by also including the estimated movement parameters in the model. A Language > Rest and Control > Rest contrast was calculated. These two contrasts were entered into a second level paired samples model in which the Language > Control contrast was calculated for the left hemispheric damage group. Only clusters surviving an uncorrected threshold of $p < 0.001$ at the voxel level with a minimum cluster size of 5 voxels are reported.

Grey and white matter loss and precise lesion location

In order to precisely locate the areas affected by the lesion in each patient, we used the 4-year old adapted LONI LPBA40 brain atlas included in the Neurodevelopmental MRI Database (Shattuck et al., 2008; Richards et al., 2015) and the lesion masks that were registered to this space. In addition, to provide a measure of grey and white matter loss, we computed an estimation of the lesion size (Tillema et al., 2008) as follows. We segmented the T1-w images into GM and WM using the 4-year-old grey and white matter segmentation priors included in the Neurodevelopmental MRI Database (Richards et al., 2015) using Unified Segmentation (Ashburner & Friston, 2005). The cerebellum and brainstem were then masked out using the manual 4-year-old atlas of the Neurodevelopmental MRI Database (Fillmore et al., 2015; Richards et al., 2015). The ratios between the total GM and WM volume in both left and right hemispheres were computed and converted to a percentage of left cerebral hemisphere loss due to stroke (Tillema et al., 2008). Recent evidence shows that although there are differences between left and right GM/WM volumes in healthy controls, these should not exceed 1% (Carne et al., 2006).

DW-MRI pre-processing

Diffusion data processing started by correcting for eddy current distortions and head motion using FMRIB's Diffusion Toolbox (FDT), which is part of the FMRIB Software Library (FSL 5.0.1, www.fmrib.ox.ac.uk/fsl/; Jenkinson et al., 2012). Subsequently, the gradient matrix was rotated (Leemans & Jones 2009). Following this, brain extraction was performed using the Brain Extraction Tool (Smith et al., 2006), which is also part of the FSL distribution. The analysis continued with the reconstruction of the diffusion tensors using the linear least-squares algorithm included in Diffusion Toolkit 0.6.2.2 (Ruopeng Wang, Van J. Wedeen, trackvis.org/dtk, Martinos Center for Biomedical Imaging, Massachusetts General Hospital). This pipeline of analysis was chosen as our acquisition parameters where fine-tuned using this procedure (see François et al., 2016).

For the control group, we directly used the tensors provided by the NIH Pediatric MRI Data Repository (already preprocessed using the standard TORTOISE pipeline, Pierpaoli et al., 2010). We chose to use the already processed tensors in order to use the data with the best quality provided by the repository. These tensors were transformed into a compatible format with Diffusion Toolkit using in-house scripts (the code is available at https://github.com/pripolles/Diffusion-Tools/).

For both patient and control data, whole-brain tractography was performed using Diffusion Toolkit 0.6.2.210 and the interpolated streamlines algorithm. Tractography was started only in voxels with an FA value greater than 0.2 and was stopped when the angle between two consecutive steps was larger than 35°. Deterministic tracking was performed by means of a two region-of-interest (ROI) approach using the TrackVis software (www.trackvis.org, Ruopeng Wang, Van J. Wedeen, TrackVis.org, Martinos Center for Biomedical Imaging, Massachusetts General Hospital).

Deterministic tractography

Given the nature of our dataset (pediatric individuals with lesions) we decided to use manual deterministic tractography to dissect the tracts of interest, as it allowed us to draw specific ROIs adapted to each individual. In other words, for each individual and tract we drawn in native space specific ROIs that took into account the neuroanatomy of each participant.

For each dataset, the three segments of AF were defined following the procedure reported by Catani et al. (2007) and also used in Lopéz-Barroso et al. (2013), Tuomiranta et al. (2014) and François et al. (2016). All ROIs were defined using the Fractional Anisotropy (FA) or RGB FA map as a reference. These FA and RGB-FA maps were generated from diffusion tensors that were reconstructed using the linear least-squares method provided in Diffusion Toolkit. The ROI for the frontal area was placed in the coronal plane, between the central fissure and the cortical projection of the tract. The ROI for the temporal area was placed in the

axial plane encompassing the fibers descending to the posterior temporal lobe through the posterior portion of the temporal stem. The third two-dimensional ROI was defined at the sagittal plane encompassing the angular and supramarginal gyri of the inferior parietal lobe. In order to virtually dissect the three segments of interest, different two-ROI combinations were applied. The streamlines going through the frontal and temporal ROIs were classified as the long segment of the AF, the streamlines connecting the temporal and parietal ROIs constituted the posterior segment of AF, and the streamlines passing through the frontal and parietal ROIs formed the anterior segment of the AF. This process was carried out for both the left and the right hemisphere. As a control, we also performed virtual *in vivo* dissections of the inferior fronto-occipital fasciculus (IFOF), inferior longitudinal fasciculus (ILF) and uncinate fasciculus (UF). These dissections were performed for both hemispheres. For each dataset, we placed three spherical ROIs (as in Ripolles et al., 2017) at the level of the anterior temporal lobe (temporal ROI), the posterior region located between the occipital and temporal lobe (occipital ROI) and the anterior floor of the external/extreme capsule (frontal ROI). In order to define each of the tracts of interest we applied, again, a two-ROI approach. The ILF was obtained by connecting the temporal and occipital ROIs (violet, see **Figure 6**). The streamlines passing through the occipital lobe and frontal ROIs were considered as part of the IFOF (blue, **Figure 6**). The frontal capsule ROI was united to the temporal ROI to delineate the UF (orange, **Figure 6**). All these ROIs were applied according to anatomical landmarks defined in the research report by Catani and Thiebaut de Schotten (2008). In addition, the exclusion of single fiber structures that do not represent part of the dissected tracts was achieved using subject-specific no-ROIs. This procedure was done for both patients and controls.

Given the location of the patients' lesions, we analyzed the volume of the AF. The volume was chosen as recent investigations revealed that this WM parameter is sensitive to individual differences (Saygin et al., 2013; Ocklenburg et al., 2014; Sreedharan et al., 2015; Vaquero et al., 2017) and that is also related to word-learning (Assaneo et al., 2019). We extracted the volume from the sum of the three segments of each hemisphere to obtain the values for complete-Left and complete-Right AF. The lateralization index was calculated [Lateralization Index = (values on the R − values on the L) / (values on the R + values on the L)] and was included in the analysis to see whether right WM reorganization had a relation with language development. The lateralization index ranges from -1 to 1: negative values represent left lateralization, values around zero symmetrical distribution, and positive values right lateralization (López-Barroso et al., 2013). As a control, we also calculated the LI for the IFOF, ILF and UF using the same procedure. We compared the LIs for the AF, ILF, IFOF and UF between controls and patients using non-parametric Wilcoxon Mann-Whitney tests. Due to the limited number of patients, confirmatory Bayesian statistical analyses were computed for all

these between group comparisons using JASP with default (JASP Team, 2018; Morey & Rouder, 2015; Rouder & Morey, 2012). We used Bayes factors (BF_{10}), which for the comparison at hand, reflect how likely data are different (e.g. a BF_{10}=3 implies that a difference between groups is 3 times more likely to be observed under the alternative hypothesis).

In order to explore the link between the volume of the AF and productive aspects of language, we performed 4 non-parametric Spearman correlations between the volume of the complete AF and (i) the two measures of phonological development (phonological complexity and proximity scores) and (ii) the two measures of expressive language complexity (MLU and L-max). To correct for multiple comparisons, the false discovery rate (FDR) was controlled at $\delta = 0.05$ where multiple tests are performed (Benjamini & Hochberg, 1995).

Resting-state-fMRI functional connectivity analysis

The rs-fMRI data were analyzed following the rationale of the tractography analyses. The already preprocessed rs-fMRI data were analyzed using the functional connectivity (CONN) toolbox v17f (Whitfield-Gabrieli & Nieto-Castanon, 2012). After preprocessing, the images were band-pass filtered to 0.008-0.09 Hz and denoised by regressing out the six motion parameters obtained during realignment and the white-matter and cerebrospinal fluid signals. Finally, data were detrended. Given the tractography results (see **Results** section) which pointed to a crucial involvement of the arcuate fasciculus in language functions in the studied patient population, we performed an rs-fMRI analysis that further confirmed these results. With this aim, we selected the two main regions connected by the arcuate fasciculus: the superior temporal gyrus (STG) and the inferior frontal gyrus (IFG, including both part opercularis and triangularis). These ROIs were extracted from the 4-year old adapted LONI LPBA40 brain atlas included in the Neurodevelopmental MRI Database (Shattuck et al., 2008; Richards et al., 2015). Data for all voxels within an ROI were averaged and one correlation per participant and hemisphere was calculated between the STG and the IFG. These correlation coefficients were converted to z-values using Fisher's r-to-z transformation. Right hemispheric z-values for each of the four correlations were subtracted from their left-hemispheric counterparts to obtain an rs-fMRI laterality index analog to the one obtained for tractography (see López-Barroso et al., 2013 for a similar analysis). Associations between these laterality indexes and (i) the two measures of phonological development (phonological complexity and proximity scores) and (ii) the two measures of expressive language complexity (MLU and L-max) were then explored using Spearman's correlations. To correct for multiple comparisons, the false discovery rate

(FDR) was controlled at $\delta = 0.05$ where multiple tests are performed (Benjamini & Hochberg, 1995).

Results

Neuropsychological testing

Peabody picture vocabulary test

The scores obtained in the Peabody vocabulary test (PPVT-III, with Spanish norms) yielded an estimate of verbal IQ which fells within normal limits with all the children having normal verbal IQ (**Figure 2A**).

NEPSY II

The scores obtained from selected subtests of the NEPSY-II were first analyzed separately for each subtest. Composite scores corresponding to four of the specific cognitive domains of the NEPSY-II (i.e. Language, Memory and Learning, Visuospatial and Sensorimotor Processing, see **Methods**) were also computed by averaging the scalar scores obtained in the target subtests from each domain. As a group, the results showed that the mean scalar scores fell within the normal range (i.e. 8-12, percentile 27-75) except for phonological processing, narrative memory, block construction, design copying and visuomotor precision subtests showing mean scores slightly below the expected values (see **Figure 3**). When considering composite scores, the mean score in the language domain, although relatively low, fell within the normal range. Similar values were obtained in both the memory and learning and the sensorimotor domains. However, the mean composite score in the visuospatial processing domain was clearly below the normal range with a mean value < 8, corresponding to percentile values 11-25.

Phonological Development

Two measures, phonological complexity (phonological mean length of utterance, pMLU) and phonological whole-word proximity (Proximity score) were obtained. We first compared the individual performance to an age-matched control group using the modified *t*-test which is specifically designed to compare a patient to a small sample of control participants (Crawford, Garthwaite, & Porter, 2010). At the individual level, only one child (L1) presented significantly lower complexity score than controls ($p = .002$, modified *t*-test, one-tailed). This patient presented a particularly poor level of performance in the measure of phonological proximity ($p < .001$, modified *t*-test, one-tailed; see **Table 2, Figures 4A, 4B, 6A, and 6B**). At

the group level, the Mann-Whitney tests comparing children with PAIS to controls did not reveal significant differences ($P > .05$).

Utterance complexity in spontaneous speech

In order to explore productive language with a specific focus on syntactic complexity, we evaluated the children expressive language complexity by using the mean length of utterance in words (MLU) and the mean length of the five longest utterances (max-L). At the individual level, L1 presented a particularly poor performance in both MLU and max-L scores ($p < .001$, modified *t*-test, one-tailed; see **Table 3** and **Figure 4C**).

Neuroimaging results

Lesion location

The lesions affected different left perisylvian language-related areas (including the inferior frontal gyrus, the middle temporal gyrus, the superior temporal gyrus and the precentral gyrus) (see **Table 4** and **Figure 6A**). The analysis of the extent of the lesions reflected by the percentage of left cerebral hemisphere loss due to stroke revealed that white matter volume loss was higher than that of grey matter in 4 out of 6 children suggesting that the lesions affected mainly white matter tissue.

fMRI Task

We obtained the functional activations from all the children using a passive story-telling task during which a short children's story was auditorily presented in 20 second-long blocks (language condition). A control condition, consisting of an acoustically-matched set of music-like stimuli, was also presented (see **Methods**); the goal of this contrast was to elicit activity related more specifically to linguistic features of the stimuli (especially phonological and semantic), rather than prosodic or more low-level auditory cues (such as duration or loudness) which were similar for the two stimulus types. The Language versus the Acoustic Control condition contrast yielded significant (but uncorrected) activity in the right middle temporal gyrus and in the right inferior frontal gyrus (see **Figure 5**, $P < 0.001$ uncorrected). No consistent activity pattern was observed in the reverse contrast (music-like condition vs. language). Note, however, that due the limited N, these results are not corrected for multiple comparisons.

Deterministic tractography

The deterministic *in vivo* dissections using the two-ROI approach revealed that for all the children with PAIS, the three segments of the AF were well preserved in the right hemisphere. Meanwhile, we were not able to dissect the left AF in most of them (L4 and L6 presented the posterior segment only, whereas L1 presented the posterior and the long segment but not the anterior one). We did not observe any substantial damage to the ventral white matter pathways (ILF, IFOF, and UF) in either hemisphere (see **Figure 6**).

Deterministic dissections in the control group revealed that the three segments of the left AF were always present. By contrast, while the anterior and posterior segments of the right AF were always present, we were not able to reconstruct the long segment of the AF in three control children. Crucially, when comparing the laterality index for the volume of the complete AF in patients and controls we found that patients presented a significantly more right-lateralized AF than controls ($U = 0$; $p < 0.001$; $BF_{10} = 147.79$). Importantly, when comparing the volume of the left and of the right AF between patients and controls, we observed significantly *reduced volume of the left AF* in patients ($U = 5$; $p < 0.009$; $BF_{10} = 36.95$) and *a larger volume of the right AF* ($U = 6$; $p < 0.013$; $BF_{10} = 6.73$) in patients as compared to controls. Moreover, in order to rule out possible group-specific differences due to the different scanning parameters and procedures used between groups, we also compared the laterality indexes of several control tracts also related to language. We found no differences between the laterality indexes of patients and controls for the ILF ($U = 18$; $p = 0.289$; $BF_{10} = 0.607$), IFOF ($U = 25$, $p = 0.814$; $BF_{10} = 0.473$) or UF ($U = 20$; $p = 0.409$; $BF_{10} = 0.574$), which further proves that our results were specific to the AF.

Brain-behaviour relationships

Given that the dorsal pathway was the most affected in patients (the laterality of the entire AF was significantly more right-lateralized in patients than in controls), we computed the laterality indices for both dorsal structural and functional data (see **Methods**). Due to the limited number of patients, confirmatory Bayesian statistical analyses were computed for all the brain-behavior correlations with the software JASP using default priors and the Bayesian Correlation module (using Kendall's tau-b; JASP Team, 2018; Morey & Rouder, 2015; Rouder & Morey, 2012). We used Bayes factors (BF_{10}), which for the comparison at hand, reflect how likely data are correlated (e.g. a BF_{10}=3 implies that a positive correlation is 3 times more likely to be observed under the alternative hypothesis).

We found a significant positive correlation ($r_s[6] = 0.94$; $p < .0001$, FDR-corrected for multiple comparisons; $BF_{10} = 5.876$) between productive aspects of language (as measured by the max-L) and the lateralization index for the volume of the complete AF (see **Figure 7A**).

This result indicated that the greater the reorganization was over the right hemisphere (i.e. higher lateralization index of AF's volume), the better productive aspects of language (higher max-L values).

Following the tractography brain-behavior results, the rs-fMRI analyses showed that the laterality values for the intrinsic connectivity strength between the STG and IFG were positively associated with productive aspects of language ($r_s[6] = 0.88$; $p < .02$; $BF_{10} = 3.43$) as measured by the MLU in spontaneous speech; see **Figure 7B**) even though these analyses did not survive the FDR correction. Nonetheless, this finding suggests that the greater the reorganization was to the right hemisphere (i.e., the greater the intrinsic functional connectivity between these two regions in the right hemisphere), the better the productive aspects of language. This pattern of results strikingly parallels the one found for the lateralization of the AF using deterministic tractography and provides converging evidence that greater right hemispheric engagement was related to better productive aspects of language in this group of children.

Discussion

In the present study, structural connectivity measures pointed toward an association between the right reorganization of the dorsal pathway and measures of expressive language development: the structural laterality indices of the right dorsal pathway predicted language production outcomes. Crucially, the structural laterality indices of the AF were significantly more right-lateralized in children with left PAIS than in a matched- group of controls while no differences were observed for the UF, ILF or IFOF.

Although all the children had normal receptive vocabulary levels and verbal IQ, they presented slightly low language production and processing outcomes as a group. The finest measure of utterance complexity in spontaneous speech (L-max) showed that half of the children presented a limited syntactical development as compared to controls. The individual results from the NEPSY-II language subtests showed that most of the children were below normative scores except for the speeded naming subtest. Besides this, most of them had below normative scores in the visuospatial processing subtests. The latter result is in line with two studies reporting impaired visuospatial processing induced by left lesions (Lidzba et al., 2006a; 2006b). Taken together, the data may indicate that the reorganization of the language network towards the right hemisphere can, in turn, impair functions originally supported by the right hemisphere, thus providing support to the so-called "crowding effect" induced by early stroke (Satz et al., 1994).

The fMRI results, although not corrected for multiple comparisons, revealed two clusters of activation over the contralesional hemisphere only, one in the right middle temporal

gyrus and the other in the right inferior frontal gyrus. Prosodic and voice processing have been recently shown to involve a dual processing stream organization with both a dorsal and a ventral pathway connecting the right posterior STG to the right IFG and premotor cortex (Sammler et al., 2015; Zäske et al., 2017; Pernet et al., 2015). Here, we used fine-grained control stimuli such that each speech sentence from the language condition had a musical-phrase correspondence with similar prosodic and acoustic features in the control condition. Therefore, these two clusters are not likely to reflect prosodic processing. Previous studies in healthy young adults have largely reported activations over these regions during active syntactic and semantic processing but with a clear left lateralization (Binder & Desai, 2011). Here, consistently with previous reports on language comprehension in children and adults with stroke (Jacola et al., 2006; François et al., 2016; Lidzba et al., 2017a, 2017b), no activation over the left hemisphere was observed. Although these results must be taken with caution (due to the small N, the presence of anesthesia, the fMRI data were not corrected for multiple comparisons), our results may suggest that both the processing of acoustical features of the voice signal, as well as high-order syntactic processing, were taking place in our group of children.

Critically, both rs-fMRI and especially DW-MRI data provided converging evidence showing that the right hemisphere can take over language functions. Successful recovery after early stroke can be associated with both intra-hemispheric perilesional and inter-hemispheric contralesional plasticity mechanisms (Dick et al., 2013; Raja-Beharelle et al., 2010). However, it is important to bear in mind that different physiological mechanisms of recovery may be triggered after arterial ischemic stroke or periventricular brain lesions which may, in turn, partly explain the different patterns of results reported here and in the study from Raja-Beharelle and colleagues (2010). Here, we found that compared to healthy controls, patients presented a smaller volume of the left AF together with a larger volume of its right homolog. These differences were transferred to the laterality index of the AF: the volume of the arcuate was more right-lateralized in patients than in controls. Interestingly, we found a clear positive association between the volume of the right AF and a measure of language production. Besides, we found an association between the laterality index of the intrinsic connectivity strength between perisylvian regions of the dorsal pathway and the MLU (although this result was not corrected for multiple comparisons). Taken together, these results indicate that reorganization of the language network over the right hemisphere can be accomplished through structural and functional hyperconnectivity between right temporal and frontal areas. An increased grey matter density in the right temporoparietal regions has been associated with a right-lateralized language network in a large group of children with drug-resistant left-sided lesional focal epilepsy (Pahs et al., 2013). The authors suggested that the size of the unaffected planum temporale may present a 'reserve capacity' for interhemispheric language reorganization in the presence of

lesions within left perisylvian regions. Additional evidence for the important role of plasticity of the right temporal cortex in the recovery of language functions came from studies conducted in left hemisphere stroke survivors with aphasia (Hope et al., 2017; Forkel et al., 2014; Lukic et al., 2017; Xing et al., 2016; Piai et al., 2017). A very recent study from Northam and colleagues (2018) gives more support to this hypothesis by showing that brain reorganization towards the right hemisphere can compensate production deficits often observed in children with left PAIS. Moreover, recent evidence exists in rats and humans showing that early lesions in the motor system can induce contralateral axonal sprouting (Liu et al., 2008; Schaechter et al., 2009). We speculate that the early disconnection of the left dorsal pathway may induce the degeneration of neurons projecting from temporal to frontal areas while triggering contralateral axonal sprouting over the right hemisphere. This contralateral reorganization mechanism may, in turn, foster contralateral increased grey matter plasticity changes reflected by structural and functional hyperconnectivity.

The present findings provide important results allowing the refinement of a recent model describing the emergence of increasingly complex linguistic functions through development (Catani & Bambini, 2014). Building upon previous neuroanatomical models of language processing (Friederici 2011, 2012; Catani et al., 2005; Hickok & Poeppel, 2007; Rauschecker & Scott, 2009), this model links the stepwise evolution of language functions to the neuro-anatomical changes occurring during early development with a specific role of the posterior and long segments of the AF, necessary for normal language development and especially in word-learning, syntactic processing and verbal working memory (Lopez-Barroso et al., 2013; Lebel & Beaulieu, 2009; Budisavljevic et al., 2015; Catani & Bambini, 2014). Nonetheless, these models remained elusive on the role of the right dorsal and ventral pathways. Prosodic cues are preferentially processed by the right hemisphere (Giraud et al., 2007; Perani et al., 2010, Zatorre & Belin, 2001) and are important for language acquisition as they may help bootstrapping language learning processes (François et al., 2017; Gervain & Werker 2013; Shukla et al., 2011; De Diego-Balaguer et al., 2015; Filippi et al., 2017). It has also been revealed that temporoparietal brain regions presented a slower maturation as compared to frontal regions in healthy infants (Leroy et al., 2011). This slow cortical maturation is paralleled by the slow maturation and high sensitivity to environmental factors of the right posterior segment of the AF (Budisavljevic et al., 2015). Our results, taken together with the previous evidence on the role of the right dorsal and ventral pathways for language processing, suggest that the right hemisphere may also play an important role in children's development and in language processing after stroke. Besides, although still under debate, recent data from children with early acquired brain lesions show that the time-window for the compensatory recruitment of homologous right cortical regions after left stroke may already close at the age of 5 years

738 (Lidzba et al., 2017a). Similarly to what has been observed in adults with aphasia (Forkel et al.,
739 2014; Hartwigsen & Saur, 2017), the right temporoparietal regions and the posterior segment of
740 the right AF may be critical for compensating the devastating effect of stroke. Therefore, the
741 enhanced involvement of the right dorsal pathway after early stroke may induce functional and
742 structural changes within a more flexible language network than lesions acquired in a highly
743 specialized functional network during adulthood (Levine et al., 2016). Future research is needed
744 to specify the role of genetic predispositions contributing to the left hemisphere specialization
745 as opposed to the neuroplastic mechanisms occurring over the right hemisphere in the face of
746 early left lesions.

747 The present study presents some limitations. The sample size is small, which is an
748 intrinsic and recurrent problem in studying rare neonatal conditions. This limitation is
749 particularly evident for the fMRI results which were not corrected for multiple comparisons. In
750 addition, the fMRI task used here is novel in this type of population and results from a control
751 group of healthy children and/or a group of adults without sedation is needed to further interpret
752 our fMRI data in terms of functional reorganization. The presence of degeneration or necrosis
753 may alter the microstructure of perilesional tissue, leading to problems in the estimation of fiber
754 orientations, especially in areas with presence of crossing fibers, which can, in turn, induce
755 artefacts in track reconstructions (Ciccarelli et al., 2006; Schonberg et al., 2006; Dell'Acqua, et
756 al., 2010; Møller et al., 2006). The use of light anesthesia to avoid movements during the MRI
757 acquisition may have influenced the functional activations as the rate of failure can be as high as
758 21% with propofol and an auditory task (Bernal et al., 2012; note, however that we were able to
759 reconstruct canonical ICA networks for each patient, see **Figure 1B**). The DWI data from the
760 NIH database were acquired with different scanning parameters which may impact the
761 comparison with the data obtained in our group patients. However, we think that this confound s
762 unlikely to be affecting our results, since the differences observed were specific to the AF and
763 not to the ventral tracts we used as a control. In addition, our sample was studied at around 4
764 years of age, and therefore is not yet fully developed (neither in terms of language abilities nor
765 in terms of brain structure/function). Other language-related deficits could appear at later stages
766 and the deficits shown here could also resolve by school age. Besides, this group of children
767 was developing in a bilingual environment (5 out of 6). The type of language input received
768 during the first years, such as the presence of co-speech gestures or the use of decontextualized
769 talk, have been shown to play an important role in the development of linguistic functions after
770 neonatal stroke specifically for those showing initial linguistic delays (Rowe et al., 2009; Demir
771 et al., 2013, 2015). This might particularly be the case for the two patients (L2 and L6) who
772 were not receiving speech therapy as previous studies have shown that interventions such as
773 music-based therapy can induce functional and structural reorganization in children (Zipse et al.,

2012). However, at present, the specific impact on bilingual experience in children with PAIS remains fairly unexplored. Taken together, these data suggest that the "catch-up" of linguistic functions previously reported once children reach elementary school (Bates, 1997) may already occur in pre-schoolers by 4 years of age, probably resulting from the enriched linguistic input provided by parents (Demir et al., 2013, 2015), caregivers and early speech stimulation programs.

In summary, we report the first 3D reconstructions of the dorsal and ventral language pathways together with fine-grained assessments of cognitive and language functions in a homogeneous group of 4-year old children who had a left PAIS. We provide evidence for an association between the structural and functional (although to a lesser extent) brain reorganization patterns toward the right hemisphere and language production in pre-school children with congenital lesions. We speculate that inter-hemispheric plasticity through structural and functional hyper-connectivity mechanisms might be crucial for positive outcomes following early lesions.

References

Almli CR, Rivkin MJ, McKinstry RC (2007) Brain Development Cooperative Group. The NIH MRI study of normal brain development (Objective-2): newborns, infants, toddlers, and preschoolers. NeuroImage 35(1):308-325.

Andersen SM, Rapcsak SZ, Beeson PM (2010) Cost function masking during normalization of brains with focal lesions: still a necessity? NeuroImage 53:78-84.

Ashburner J, Friston KJ (2005) Unified segmentation. NeuroImage 26:839-851.

Assaneo MF, Ripolles P, Orpella J, Lin WM, de Diego-Balaguer R, Poeppel D (2019) Spontaneous synchronization to speech reveals neural mechanisms facilitating language learning. Nat Neurosci 22(4):627-632.

Bajada CJ, Lambon Ralph MA, Cloutman, LL (2015) Transport for language south of the Sylvian fissure: The routes and history of the main tracts and stations in the ventral language network. Cortex 69:141-51.

Ballantyne AO, Spilkin AM, Hesselink J, Trauner DA (2008) Plasticity in the developing brain: intellectual, language and academic functions in children with ischaemic perinatal stroke. Brain 131(11):2975-2985.

Bates, E (1997) Origins of language disorders: A comparative approach. Developmental Neuropsychology 13(3):447-476.

807 Bates E, Reilly J, Wulfeck B, Dronkers N, Opie M, Fenson J, Kriz S, Jeffries R, Miller
808 L, Herbst K (2001) Differential effects of unilateral lesions on language production in children
809 and adults. Brain Lang 79(2):223-265.

810 Bell AJ, Sejnowski TJ (1995) An information-maximization approach to blind
811 separation and blind deconvolution. Neural computation 7(6):1129-1159.

812 Benjamini Y, Hochberg Y (1995) Controlling the false discovery rate: a practical and
813 powerful approach to multiple testing. Journal of the royal statistical society. Series B
814 (Methodological):289-300.

815 Bernal B, Grossman S, Gonzalez R, Altman N (2012) FMRI under sedation: what is the
816 best choice in children? J Clin Med Res 4(6):363-370.

817 Binder JR, Desai RH (2011) The neurobiology of semantic memory. Trends Cogn Sci
818 15(11):527-536.

819 Blasi A, Mercure E, Lloyd-Fox S, Thomson A, Brammer M, Sauter D, Deeley Q,
820 Barker GJ, Renvall V, Deoni S, Gasston D, Williams SC, Johnson MH, Simmons A, Murphy
821 DG (2011) Early specialization for voice and emotion processing in the infant brain. Curr Biol
822 21(14):1220-1224.

823 Bosch, L. (2004) Evaluación fonológica del habla infantil. Barcelona: Masson.

824 Boveroux P, Vanhaudenhuyse A, Bruno MA Noirhomme Q, Lauwick S, Luxen A,
825 Degueldre C, Plenevaux A, Schnakers C, Phillips C, Brichant JF, Bonhomme V, Maquet P,
826 Greicius MD, Laureys S, Boly M (2010) Breakdown of within- and between-network resting
827 state functional magnetic resonance imaging connectivity during propofol-induced loss of
828 consciousness. Anesthesiology 113:1038-1053.

829 Brauer J, Anwander A, Perani D, Friederici AD (2013) Dorsal and ventral pathways in
830 language development. Brain Lang 127:289-295.

831 Brett M, Leff AP, Rorden C, Ashburner J (2001) Spatial normalization of brain images
832 with focal lesions using cost function masking. NeuroImage 14:486-500.

833 Brown TT, Lugar HM, Coalson RS, Miezin FM, Petersen SE, Schlagga, BL (2005)
834 Developmental changes in human cerebral functional organization for word generation. Cereb
835 Cortex 15(3):275-290.

836 Budisavljevic S, Dell'Acqua F, Rijsdijk FV, Kane F, Picchioni M, McGuire P,
837 Toulopoulou T, Georgiades A, Kalidindi S, Kravariti E, Murray RM, Murphy DG, Craig MC,
838 Catani M (2015) Age-Related Differences and Heritability of the Perisylvian Language
839 Networks. J Neurosci 35(37):12625-12634.

840 Calhoun VD, Adali T, McGinty VB, Pekar JJ, Watson TD, Pearlson GD (2001) fMRI
841 activation in a visual-perception task: network of areas detected using the general linear model
842 and independent components analysis. NeuroImage 14(5):1080-1088.

843 Calhoun VD, Adali T, Pearlson GD, Pekar, JJ (2001) A method for making group
844 inferences from functional MRI data using independent component analysis. Human brain
845 mapping 14(3):140-151.

846 Carne RP, Vogrin S, Litewka L, Cook MJ (2006) Cerebral cortex: an MRI-based study
847 of volume and variance with age and sex. J Clin Neurosci 13(1):60-72.

848 Catani M, Jones DK, Donato R, Ffytche DH (2003) Occipito-temporal connections in
849 the human brain. Brain 126:2093-2107.

850 Catani M, Jones DK, Fytche DH (2005) Perisylvian language networks of the human
851 brain. Ann Neurol 57:8-16.

852 Catani M, Allin M, Husain M, Pugliese L, Mesulam M, Murray R, Jones DK (2007)
853 Symmetries in human brain language pathways predict verbal recall. Proc Natl Acad Sci USA
854 104:17163-17168.

855 Catani M, Thiebaut de Schotten M (2008) A diffusion tensor imaging tractography atlas
856 for virtual in vivo dissections. Cortex 44(8):1105-1132.

857 Catani M, Bambini V (2014) A model for social communication and language evolution
858 and development (SCALED). Curr Opin Neurobiol 28:165-171.

859 Ciccarelli O, Behrens TE, Altmann DR, Orrell RW, Howard RS, Johansen-Berg H,
860 Mille, DH, Matthews PM, Thompson AJ (2006) Probabilistic diffusion tractography: a potential
861 tool to assess the rate of disease progression in amyotrophic lateral sclerosis. Brain 129:1859-
862 1871.

863 Crawford JR, Garthwaite PH, Porter S (2010) Point and interval estimates of effect
864 sizes for the case-controls design in neuropsychology: rationale, methods, implementations, and
865 proposed reporting standards. Cogn Neuropsychol 27(3):245-260.

866 de Diego-Balaguer R, Rodríguez-Fornells A, Bachoud-Lévi AC (2015) Prosodic cues
867 enhance rule learning by changing speech segmentation mechanisms. Frontiers in psychology
868 6:1478.

869 Dehaene-Lambertz G, Dehaene S, Hertz-Pannier L (2002) Functional neuroimaging of
870 speech perception in infants. Science 298:2013-2015.

Dehaene-Lambertz G, Hertz-Pannier L, Dubois J, Mériaux S, Roche A, Sigman M, Dehaene S (2006) Functional organization of perisylvian activation during presentation of sentences in preverbal infants. Proc Natl Acad Sci USA 103(38):14240-14245.

Dehaene-Lambertz G, Spelke ES (2015) The Infancy of the Human Brain. Neuron 88(1):93-109.

Dell'acqua F, Scifo P, Rizzo G, Catani M, Simmons A, Scotti G, Fazio F (2010) A modified damped Richardson-Lucy algorithm to reduce isotropic background effects in spherical deconvolution. NeuroImage 49(2):1446-1458.

Demir Ö, Fisher JA, Goldin-Meadow S, Levine SC (2013) Narrative processing in typically developing children and children with early unilateral brain injury: seeing gesture matters. Dev Psychol 50(3):815-828.

Demir, ÖE, Rowe ML, Heller G, Goldin-Meadow S, Levine SC (2015) Vocabulary, syntax, and narrative development in typically developing children and children with early unilateral brain injury: early parental talk about the "there-and-then" matters. Dev Psychol 51(2):161-175.

Dick AS, Raja Beharelle A, Solodkin A, Small SL (2013) Inter-hemispheric functional connectivity following prenatal or perinatal brain injury predicts receptive language outcome. J Neurosci 33(13):5612-5625.

DiFrancesco MW, Robertson SA, Karunanayaka P, Holland SK (2013) BOLD fMRI in infants under sedation: Comparing the impact of pentobarbital and propofol on auditory and language activation. J Magn Reson Imaging 38(5):1184-1195.

Dunn LM, Dunn LM, Arribas D (1997) PPVT-III. Peabody picture vocabulary test. Spanish adaptation.

Fernández Vázquez M, Aguado Alonso, G (2007) Medidas del desarrollo típico de la morfosintaxis para la evaluación del lenguaje espontáneo de niños hispanohablantes. Revista de Logopedia, Foniatría y Audiología 27(3):140-152.

Filippi P, Laaha S, Fitch WT (2017) Utterance-final position and pitch marking aid word learning in school-age children. Royal Society open science 4(8):161035.

Fillmore PT, Richards JE, Phillips-Meek MC, Cryer A, Stevens M (2015) Stereotaxic Magnetic Resonance Imaging Brain Atlases for Infants from 3 to 12 Months. Dev Neurosci 37(6):515-532.

902 Forkel SJ, Thiebaut de Schotten SM, Dell'Acqua F, Kalra L, Murphy DG, Williams SC,
903 Catani M (2014) Anatomical predictors of aphasia recovery: a tractography study of bilateral
904 perisylvian language networks. Brain 137:2027-2039.

905 François, C., Ripollés, P., Bosch, L., Garcia-Alix, A., Muchart, J., Sierpowska, J., Fons,
906 C., Solé, J., Rebollo, M., Gaitán, H., Rodriguez-Fornells, A. (2016) Language learning and
907 brain reorganization in a 3.5-year-old child with left perinatal stroke revealed using structural
908 and functional connectivity. Cortex 77:95-118.

909 François, C., Teixidó, M., Takerkart, S., Agut, T., Bosch, L., Rodriguez-Fornells, A.
910 (2017) Enhanced Neonatal Brain Responses To Sung Streams Predict Vocabulary Outcomes By
911 Age 18 Months. Scientific Reports 7(1):12451.

912 Friederici AD (2009) Pathways to language: fiber tracts in the human brain. Trends
913 Cognit Sci 13:175-181.

914 Friederici AD (2011) The brain basis of language processing: from structure to
915 function. Physiol Rev 91(4):1357-1392.

916 Friederici AD (2012) Language development and the ontogeny of the dorsal pathway.
917 Front Evol Neurosci 4:3.

918 Gervain J, Werker JF (2013) Prosody cues word order in 7-month-old bilingual infants.
919 Nat Commun 4:1490.

920 Giraud AL, Kleinschmidt A, Poeppel D, Lund TE, Frackowiak RS, Laufs H (2007)
921 Endogenous cortical rhythms determine cerebral specialization for speech perception and
922 production. Neuron 56(6):1127-1134.

923 Hartwigsen G, Saur D (2017) Neuroimaging of stroke recovery from aphasia–Insights
924 into plasticity of the human language network. NeuroImage S1053-8119(17):31000-31005.

925 Hickok G, Poeppel D (2007) The cortical organization of speech processing. Nat Rev
926 Neurosci 8:393-402.

927 Hope TM, Lef, AP, Prejawa S, Bruce R, Haigh Z, Lim L, Ramsden S, Oberhuber M,
928 Ludersdorfer P, Crinion J, Seghier ML, Price CJ (2017) Right hemisphere structural adaptation
929 and changing language skills years after left hemisphere stroke. Brain 140(6):1718-1728.

930 Ingram D (2002) The measurement of whole-word productions. J Child Lang 29:713-
931 733.

932 Jacola LM, Schapiro MB, Schmithorst VJ, Byars AW, Strawsburg RH, Szaflarski JP,
933 Plante E, Holland SK (2006) Functional magnetic resonance imaging reveals atypical language

organization in children following perinatal left middle cerebral artery stroke. Neuropediatrics 37(1):46-52.

JASP Team (2018) JASP (Version 0.8.6) [Computer software].

Jenkinson M, Beckmann CF, Behrens TE, Woolrich MW, Smith SM (2012) FSL. NeuroImage 62(2):782-790.

Kerssens C, Hamann S, Peltier S, Hu XP, Byas-Smith MG, Sebel PS (2005) Attenuated brain response to auditory word stimulation with sevoflurane: a functional magnetic resonance imaging study in humans. Anesthesiology 103:11-19.

Korkman M, Kirk U, Kemp S (2007) NEPSY-II. San Antonio, TX: Pearson. [Spanish adaptation by Universidad de Sevilla, FIVAN y Departamento I+D Pearson Clinical & Talent Assessment (2014). Madrid: Pearson Publ.]

Lai G, Schneider HD, Schwarzenberger JC, Hirsch J (2011) Speech stimulation during functional MR imaging as a potential indicator of autism. Radiology 260:521-530.

Lebel C, Beaulieu C (2009) Lateralization of the arcuate fasciculus from childhood to adulthood and its relation to cognitive abilities in children. Human Brain Mapping 30(11):3563-3573.

Leemans A, Jones DK (2009) The B-matrix must be rotated when correcting for subject motion in DTI data. Magn Reson Med 61(6):1336-1349.

Leroy F, Glasel H, Dubois J, Hertz-Pannier L, Thirion B, Mangin JF, Dehaene-Lambertz G (2011) Early maturation of the linguistic dorsal pathway in human infants. J. Neurosci 31(4):1500-1506.

Levine SC, Beharelle AR, Demir OE, Small SL (2016) Perinatal focal brain injury: Scope and limits of plasticity for language e functions. The neurobiology of language, (Eds: Hickok, G, Small, S.). Academic Press, London, England p. 969-979.

Liberman AM, Mattingly IG (1985) The motor theory of speech perception revised. Cognition 21(1):1-36.

Lidzba K, Staudt M, Wilke M, Grodd W, Krägeloh-Mann I. (2006a) Lesion-induced right-hemispheric language and organization of nonverbal functions. Neuroreport 17(9):929-933.

Lidzba K, Staudt M, Wilke M, Krägeloh-Mann I. (2006b) Visuospatial deficits in patients with early left-hemispheric lesions and functional reorganization of language: consequence of lesion or reorganization? Neuropsychologia 44(7):1088-1094.

966 Lidzba K, Küpper H, Kluger G, Staudt M (2017a) The time window for successful
967 right-hemispheric language reorganization in children. Eur J Paediatr Neurol 21(5):715-721.

968 Lidzba K, deHaan B, Wilke M, Krägeloh-Mann I, Staudt M (2017b) Lesion
969 characteristics driving right-hemispheric language reorganization in congenital left-hemispheric
970 brain damage. Brain Lang 173:1-9.

971 Liu Z, Li Y, Zhang X, Savant-Bhonsale S, Chopp M (2008) Contralesional axonal
972 remodeling of the corticospinal system in adult rats after stroke and bone marrow stromal cell
973 treatment. Stroke 39(9):2571-2577.

974 Liu F, Patel AD, Fourcin A, Stewart L (2010) Intonation processing in congenital
975 amusia: discrimination, identification and imitation. Brain 133:1682-1693.

976 Lopez-Barroso D, Catani M, Ripolles P, Dell'acqua F, Rodriguez-Fornells A, de Diego-
977 Balaguer R (2013) Word learning is mediated by the left arcuate fasciculus. Proc Natl Acad Sci
978 USA 110(32):13168-13173.

979 Lukic S, Barbieri E, Wang X, Caplan D, Kiran S, Rapp B, Parrish TB, Thompson CK
980 (2017) Right Hemisphere Grey Matter Volume and Language Functions in Stroke Aphasia.
981 Neural plasticity 2017:5601509.

982 Meyer L, Cunitz K, Obleser J, Friederici AD (2014) Sentence processing and verbal
983 working memory in a white-matter-disconnection patient. Neuropsychologia, 61:190-196.

984 Møller M, Frandsen J, Andersen G, Gjedde A, Vestergaard-Poulsen P, Østergaard L
985 (2007) Dynamic changes in cortico spinal tracts after stroke detected by fibre tracking. J Neurol
986 Neurosurg Psychiatry 78(6):587-592.

987 Morey RD, Rouder JN (2015) BayesFactor (Version 0.9.10-2) [Computer software].

988 Nelson KB, Lynch JK (2004) Stroke in newborn infants. Lancet Neurol 3(3):150-158.

989 Northam G, Adler S, Eschmann KCJ, Chong WK, Cowan FM, Baldeweg T (2018)
990 Developmental conduction aphasia after neonatal stroke. Annals of Neurology 83(4):664-675.

991 Ocklenburg S, Schlaffke L, Hugdahl K, Westerhausen R (2014) From structure to
992 function in the lateralized brain: how structural properties of the arcuate and uncinate fasciculus
993 are associated with dichotic listening performance. Neurosci Lett 580:32-36.

994 Pahs G, Rankin P, Helen Cross J, Croft L, Northam GB, Liegeois F, Greenway S,
995 Harrison S, Vargha-Khadem F, Baldeweg T (2013) Asymmetry of planum temporale constrains
996 interhemispheric language plasticity in children with focal epilepsy. Brain 136(Pt 10): 3163-
997 3175.

998 Pani E, Zheng X, Wang J, Norton A, Schlaug G (2016) Right hemisphere structures
999 predict poststroke speech fluency. Neurology 86(17):1574-1581.

1000 Patel AD, Peretz I, Tramo M, Labreque R (1998) Processing prosodic and musical
1001 patterns: a neuropsychological investigation. Brain Lang 61:123-144.

1002 Perani D, Saccuman MC, Scifo P, Spada D, Andreolli G, Rovelli R, Baldoli C, Koelsch
1003 S (2010) Functional specializations for music processing in the human newborn brain. Proc Natl
1004 Acad Sci USA 107:4758-4763.

1005 Perani D, Saccuman MC, Scifo P, Anwander A, Spada D, Baldoli C, Poloniato A,
1006 Lohmann G, Friederici AD (2011) Neural language networks at birth. Proc Natl Acad Sci USA
1007 108(38):16056-16061.

1008 Pernet CR, McAleer P, Latinus M, Gorgolewski KJ, Charest I, Bestelmeyer PE, Watson
1009 RH, Fleming D, Crabbe F, Valdes-Sosa M, Belin P (2015) The human voice areas: Spatial
1010 organization and inter-individual variability in temporal and extra-temporal cortices.
1011 NeuroImage 119:164-174.

1012 Piai V, Meyer L, Dronkers NF, Knight RT (2017) Neuroplasticity of language in left -
1013 hemisphere stroke: Evidence linking subsecond electrophysiology and structural connections.
1014 Human brain mapping 38(6):3151-3162.

1015 Pierpaoli C, Walker L, Irfanoglu MO, Barnett A, Basser P, Chang LC, Koai C, Pajevic
1016 S, Rohde G, Sarlls J, Wu M (2010) TORTOISE: an integrated software package for processing
1017 of diffusion MRI data. Book TORTOISE: an integrated software package for processing of
1018 diffusion MRI data (Editor ed^ eds), 18, 1597.

1019 Price CJ (2012) A review and synthesis of the first 20 years of PET and fMRI studies of
1020 heard speech, spoken language and reading. NeuroImage 62:816-847.

1021 Raja-Beharelle A, Dick AS, Josse G, Solodkin A, Huttenlocher PR, Levine SC, Small
1022 SL (2010) Left hemisphere regions are critical for language in the face of early left focal brain
1023 injury. Brain 133(Pt6):1707-1716.

1024 Rauschecker JP, Scott SK (2009) Maps and streams in the auditory cortex: nonhuman
1025 primates illuminate human speech processing. Nat Neurosci 12(6):718-724.

1026 Reilly JS, Wasserman S, Appelbaum M (2013) Later language development in
1027 narratives in children with perinatal stroke. Dev Sci 16:67-83.

1028 Richards JE, Sanchez C, Phillips-Meek M, Xie W. (2015) A database of age-
1029 appropriate average MRI templates. NeuroImage 124(Pt B):1254-1259.

1030 Richter W, Richter M (2003) The shape of the fMRI BOLD response in children and
1031 adults changes systematically with age. NeuroImage 20:1122-1131.

1032 Ripollés, P., Marco-Pallarés, J., de Diego-Balaguer, R., Miró, J., Falip, M., Juncadella,
1033 M., Rubio, F., Rodriguez-Fornells, A. (2012) Analysis of automated methods for spatial
1034 normalization of lesioned brains. NeuroImage 60(2):1296-1306.

1035 Ripollés, P., Biel, D., Peñaloza, C., Kaufmann, J., Marco-Pallarés, J., Noesselt, T.,
1036 Rodríguez-Fornells, A. (2017) Strength of Temporal White Matter Pathways Predicts Semantic
1037 Learning. J Neurosci 37(46):11101-11113.

1038 Rodríguez-Fornells, A., Cunillera, T., Mestres-Missé, A., de Diego-Balaguer, R. (2009)
1039 Neurophysiological mechanisms involved in language learning in adults. Philosophical
1040 Transaction of the Royal Society B: Biological Science 364:3711-3735.

1041 Rojkova K, Volle E, Urbanski M, Humbert F, Dell'Acqua F, e Schotten, MT (2016)
1042 Atlasing the frontal lobe connections and their variability due to age and education: a spherical
1043 deconvolution tractography study. Brain Structure and Function 221(3):1751-1766.

1044 Rouder JN, Morey RD (2012) Default Bayes Factors for Model Selection in
1045 Regression. Multivariate Behav Res 47:877-903.

1046 Rowe ML, Levine SC, Fisher JA, Goldin-Meadow S (2009) Does linguistic input play
1047 the same role in language learning for children with and without early brain injury? Dev
1048 Psychol 45(1):90-102.

1049 Sammler D, Grosbras MH, Anwander A, Bestelmeyer PE, Belin P (2015) Dorsal and
1050 Ventral Pathways for Prosody. Curr Biol 25(23):3079-3085.

1051 Sanchez CE, Richards JE, Almli CR (2011) Neurodevelopmental MRI brain templates
1052 for children from 2 weeks to 4 years of age. Dev Psychobiol 54(1):77-91.

1053 Satz P, Strauss E, Hunter M, Wada J (1994) Re-examination of the crowding
1054 hypothesis: Effects of age of onset. Neuropsychology 8(2):255-262.

1055 Saur D, Kreher BW, Schnell S, Kummerer D, Kellmeyer P, Vry MS, Umarova R,
1056 Musso M, Glauche V, Abel S, Huber W, Rijntjes M, Hennig J, Weiller C (2008) Ventral and
1057 dorsal pathways for language. Proc Natl Acad Sci USA 105:18035-18040.

1058 Saygin ZM, Norton ES, Osher DE, Beach SD, Cyr AB, Ozernov-Palchik O, Yendiki A,
1059 Fischl B, Gaab N, Gabrieli JD (2013) Tracking the roots of reading ability: white matter volume
1060 and integrity correlate with phonological awareness in pre-reading and early-reading
1061 kindergarten children. J Neurosci 33(33):13251-13258.

1062 Schaechter JD, Fricker ZP, Perdue KL, Helmer KG, Vangel MG, Greve DN, Makris N
1063 (2009) Microstructural status of ipsilesional and contralesional corticospinal tract correlates
1064 with motor skill in chronic stroke patients. Human brain mapping 30(11):3461-3474.

1065 Schlaug G (2018) Even when right is all that's left: there are still more options for
1066 recovery from aphasia. Annals of Neurology 83(4):661-663.

1067 Schonberg T, Pianka P, Hendler T, Pasternak O, Assaf Y (2006). Characterization of
1068 displaced white matter by brain tumors using combined DTI and fMRI. Neuroimage
1069 30(4):1100-1111.

1070 Shattuck DW, Mirza M, Adisetiyo V, Hojatkashani C, Salamon G, Narr KL, Poldrack
1071 RA, Bilder RM, Toga AW (2008) Construction of a 3D probabilistic atlas of human cortical
1072 structures. NeuroImage 39(3):1064-1080.

1073 Shukla M, White KS, Aslin RN (2011) Prosody guides the rapid mapping of auditory
1074 word forms onto visual objects in 6-mo-old infants. Proc Natl Acad Sci USA 108(15):6038-
1075 6043.

1076 Shultz S, Vouloumanos A, Bennett RH, Pelphrey K (2014) Neural specialization for
1077 speech in the first months of life. Dev Sci 17(5):766-774.

1078 Smith SM, Jenkinson M, Johansen-Berg H, Rueckert D, Nichols TE, Mackay CE,
1079 Watkins KE, Ciccarelli O, Cader MZ, Matthews PM, Behrens TE (2006) Tract-based spatial
1080 statistics: Voxel wise analysis of multi-subject diffusion data. NeuroImage 31:1487-1505.

1081 Souweidane MM, Kim KH, McDowall R, Ruge MI, Lis E, Krol G, Hirsch J (1999)
1082 Brain mapping in sedated infants and young children with passive-functional magnetic
1083 resonance imaging. Pediatr Neurosurg 30(2):86-92.

1084 Sreedharan RM, Menon AC, James JS, Kesavadas C, Thomas SV (2015) Arcuate
1085 fasciculus laterality by diffusion tensor imaging correlates with language laterality by functional
1086 MRI in preadolescent children. Neuroradiology 57(3):291-297.

1087 Staudt M, Lidzba K, Grodd W, Wildgruber D, Erb M, Krägeloh-Mann I (2002) Right-
1088 hemispheric organization of language following early left-sided brain lesions: functional MRI
1089 topography. NeuroImage 16(4):954-967.

1090 Stiles J, Reilly J, Paul B, Moses P (2005) Cognitive development following early brain
1091 injury: evidence for neural adaptation. Trends in cognitive sciences 9(3):136-143.

1092 Szaflarski JP, Schmithorst VJ, Altaye M, Byars AW, Ret J, Plante E, Holland SK
1093 (2006) A longitudinal functional magnetic resonance imaging study of language development in
1094 children 5 to 11 years old. Annals of Neurology 59(5):796-807.

1095 Telkemeyer S, Rossi S, Koch SP, Nierhaus T, Steinbrink J, Poeppel D, Obrig H,
1096 Wartenburger I (2009) Sensitivity of newborn auditory cortex to the temporal structure of
1097 sounds. J Neurosci 29(47):14726-14733.

1098 Thiebaut de Schotten M, Ffytche DH, Bizzi A, Dell'Acqua F, Allin M, Walshe M,
1099 Murray R, Williams SC, Murphy DG, Catani M (2011) Atlasing Location, Asymmetry and
1100 Inter-Subject Variability of White Matter Tracts in the Human Brain with MR Diffusion
1101 Tractography Neuroimage 54:49-59.

1102 Tillema JM, Byars AW, Jacola LM, Schapiro MB, Schmithorst VJ, Szaflarski JP,
1103 Holland SK (2008) Cortical reorganization of language functioning following perinatal left
1104 MCA stroke. Brain Lang 106(3):184-194.

1105 Tivarus ME, Starling SJ, Newport EL, Langfitt JT (2012) Homotopic language
1106 reorganization in the right hemisphere after early left hemisphere injury. Brain Lang 123(1):1-
1107 10.

1108 Tuomiranta LM, Camara E, Froudist WS, Ripolles P, Saunavaara JP, Parkkola R,
1109 Martin N, Rodriguez-Fornells A, Laine M (2014) Hidden word learning capacity through
1110 orthography in aphasia. Cortex 50:174-191.

1111 Vaquero L, Rodríguez-Fornells A, Reiterer SM (2017) The Left, The Better: White-
1112 Matter Brain Integrity Predicts Foreign Language Imitation Ability. Cereb Cortex 27(8):3906-
1113 3917.

1114 Vandermosten M, Boets B, Poelmans H, Sunaert S, Wouters J, Ghesquiere P (2012). A
1115 tractography study in dyslexia: neuroanatomic correlates of orthographic, phonological and
1116 speech processing. Brain 135(3):935-948.

1117 Westmacott R, MacGregor D, Askalan R (2009) Late emergence of cognitive deficits
1118 after unilateral neonatal stroke. Stroke 40(6):2012-2019.

1119 Westmacott R, Askalan R, MacGregor D, Anderson P, Deveber G (2010) Cognitive
1120 outcome following unilateral arterial ischaemic stroke in childhood: Effects of age at stroke and
1121 lesion location. Developmental Medicine & Child Neurology 52:386-393.

1122 Whitfield-Gabrieli S, Nieto-Castanon A (2012) Conn: a functional connectivity toolbox
1123 for correlated and anticorrelated brain networks. Brain Connectivity 2(3):125-141.

1124 Xing S, Lacey EH, Skipper-Kallal LM, Jiang X, Harris-Love ML, Zeng J, Turkeltaub
1125 PE (2016) Right hemisphere grey matter structure and language outcomes in chronic left
1126 hemisphere stroke. Brain 139(Pt 1):227-241.

Yasuda N, Lockhart SH, Eger EI 2nd, Weiskopf RB, Liu J, Laster M, Taheri S, Peterson NA (1991) Comparison of kinetics of sevoflurane and isoflurane in humans. Anesth Analg 72(3):316-324.

Zäske R, Awwad Shiekh Hasan B, Belin P (2017) It doesn't matter what you say: FMRI correlates of voice learning and recognition independent of speech content. Cortex 94:100-112.

Zatorre RJ, Belin P (2001) Spectral and temporal processing in human auditory cortex. Cereb Cortex 11(10):946-953.

Zhang J, Evans A, Hermoye L, Lee SK, Wakana S, Zhang W, Donohue P, Miller MI, Huang H, Wang X, van Zijl PC, Mori, S (2007) Evidence of slow maturation of the superior longitudinal fasciculus in early childhood by diffusion tensor imaging. NeuroImage 38(2):239-247.

Zipse L, Norton A, Marchina S, Schlaug G. (2012) When right is all that is left: plasticity of right-hemisphere tracts in a young aphasic patient. Annals of the New York Academy of Sciences 1252(1):237-245.

Legends

Figure 1. (A) Depiction of the structural lesions in native space using a T1-w axial image. The lesions can be seen as hypo-intense areas and are highlighted with a red circle. Neurological convention is used. (B) Individual Default-Mode Networks for each patient, obtained using Group Spatial ICA on the resting state data (see **Methods**). Individual data is in z-scores ($p < 0.05$, uncorrected) and presented over each patient´s T1 registered to a common space (4-year-old MRI brain template obtained from the Neurodevelopmental MRI Database; see **Methods**). This was done as a demonstration of data quality, given that propofol can reduce connectivity in cortical areas of significance for the current study (Boveroux et al., 2010). On the right, the average DMN for all patients is depicted (using *t*-values, ($p < 0.01$, uncorrected) over a canonical 4-year-old MRI brain template. (C) Probability templates for the left arcuate (anterior, posterior and long segmente) were extracted from the Tractotron atlas (Rojkova et al., 2016; Thiebeaut de Schotten et al., 2011), thresholded at a 80% (only voxels having a 80% probability of being part of the AF according to the atlas are shown) and registered to a common space (the 4 year-old MRI brain template obtained from the Neurodevelopmental MRI Database). For each patient, here we depict the arcuate probabilistic atlas (in red), the lesion (in blue) and the overlap between them (in pink) over a sagittal slice of the left hemisphere. Neurological convention is used. L, left hemisphere.

Figure 2. Cognitive outcomes. (A) Results of the PPVT-III test for each patient. The bars show the mean and SD. (B) Means and standard deviations barplots of the composite scores from the NEPSY-II. The grey slots indicate normative scores range (8-12).

Figure 3. Means and standard deviations boxplots in the different subtests of the NEPSY-II (CI = comprehension of instruction; BPNI= body-part naming and identification; WG = word generation; PP = phonological processing; SN = speeded naming; MD = memory for designs; NM = narrative memory; SR = sentence repetition; BC = block construction; DC= design copying; IHP = imitating hand positions, VMP = visuomotor precision) grouped in domains (green = language; orange = memory and learning; violet = visuospatial processing, blue = sensorimotor processing). The grey slot indicates normative scores range (8-12).

Figure 4. Expressive language measures. Means and standard deviations boxplots for children with PAIS and controls, for proximity and complexity scores. The graphs represent individual scores for the Proximity score (A) and for the pMLU scores (B) and from the referent group (N = 50), the group mean value (in black) and the score from each patient (in red). [Maximum score for the pMLU score (complexity of the segmental structure of the words (consonants) is 8.31); maximum score for Proximity score is 1]. (C) Utterance complexity in spontaneous speech with the Mean Length of Utterance in words (MLU) and the MLU of the five longest utterances (max-L) for each patient. The grey slots indicate the scores range from an age-matched control group of N = 50 Spanish-speaking children at age 4 (Fernández & Aguado, 2007).

Figure 5. fMRI activation in the passive listening task for the Language vs. Control contrast in patients. Two significant clusters with enhanced fMRI activity are found over the right inferior frontal and middle temporal gyri. Color-coded results are shown in yellow and at a $p < .001$, in red at $p < .005$, in green at $p < .01$ and in blue at $p < .05$ uncorrected threshold with 5 voxels of cluster extent, over the Neurodevelopmental MRI Database 4-year-old template from Richards and colleagues (2015). Neurological convention is used.

Figure 6. Deterministic tractography. DTI *in-vivo* dissections of the four tracts of interest AF/ILF/UF/IFOF shown in native space on the T1-w images in each patient (A) and four controls (B). Neurological convention is used. The two-ROI approach revealed that for all the children with a left PAIS (A), the three segments of the AF were well preserved in the right hemisphere. Meanwhile, we were not able to dissect the left AF in most of them (L4 and L6 presented the posterior segment only, whereas L1 presented the posterior and the long segment but not the anterior one). We did not observe any substantial damage for the ventral white matter pathways (ILF, IFOF, and UF) in either hemisphere. By contrast, the three segments of the left AF were always present in control children (B). However, while the anterior and posterior segments of the right AF were always present in these children, we were not able to reconstruct the long segment of the AF in three controls.

Figure 7. (A) Correlation between DTI properties extracted from the manual reconstruction of the arcuate fasciculus bilaterally and productive aspects of language. The positive correlation between the lateralization index for the volume of the complete right AF and the maximum length of utterance (L-max) is shown. Lateralization index: values closer to -1 mean lateralization to the left, values around 0 represent a symmetrical distribution, values closer to 1 mean lateralization to the right. This result evidences that the more lateralized to the right is the integrity of the AF, the better the productive aspects of language. (B) Correlation between rs-fMRI laterality indexes and productive aspects of language. The scatterplot shows the positive Spearman correlation between the lateralization index for the STG-IFG laterality index and the mean length of utterance. This result evidences that the more lateralized to the right the intrinsic connectivity between the regions connected by the AF, the better the productive aspects of language. A 3D render of the 4-year-old template is displayed with the ROIs used in this analysis. IFG: Inferior frontal gyrus; STG: Superior temporal gyrus. Correlation index and *P*-values are displayed.

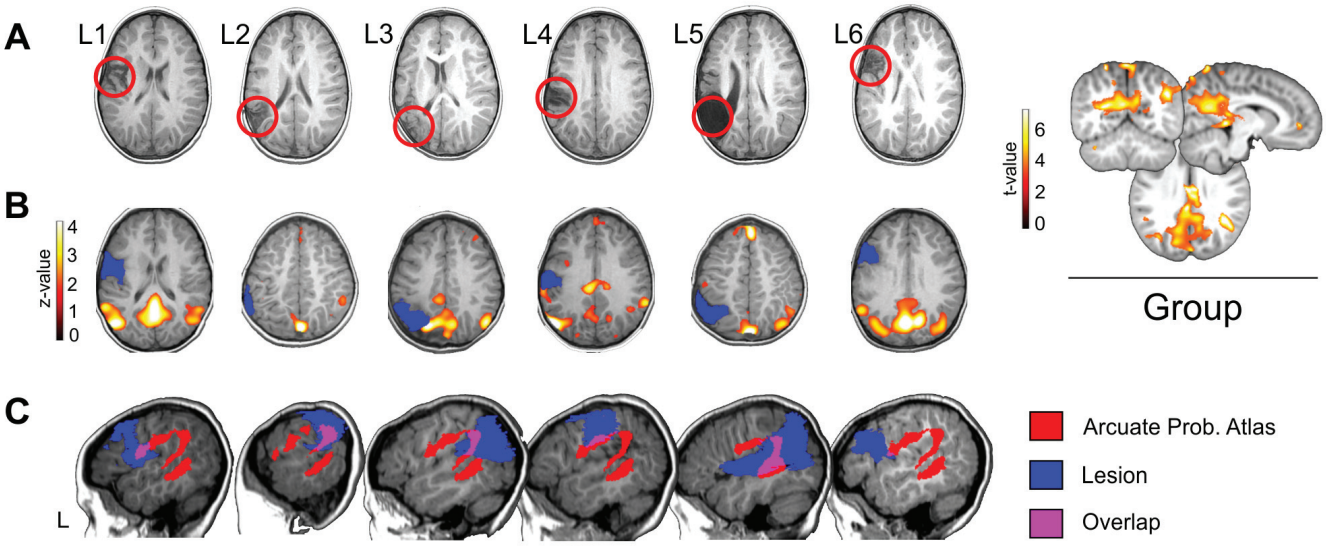

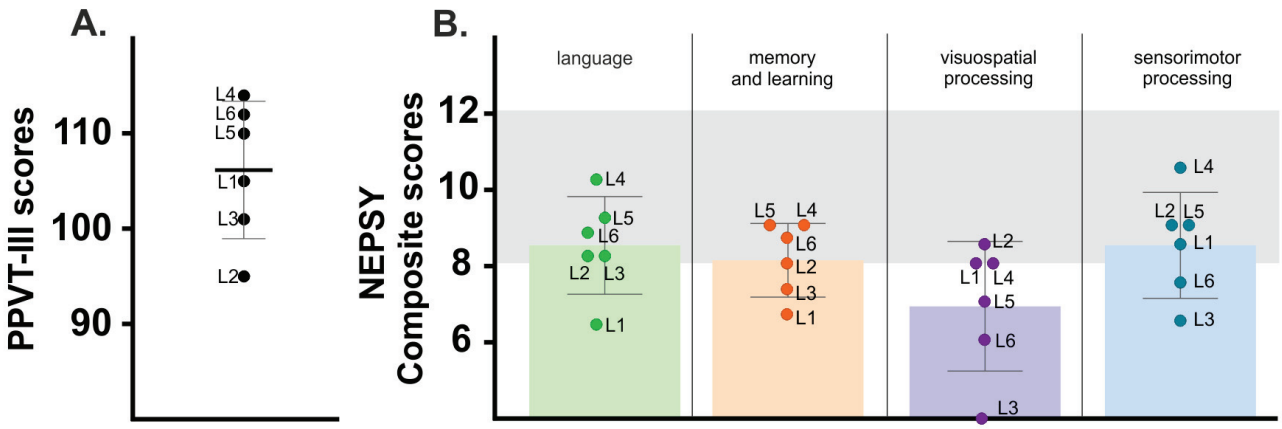

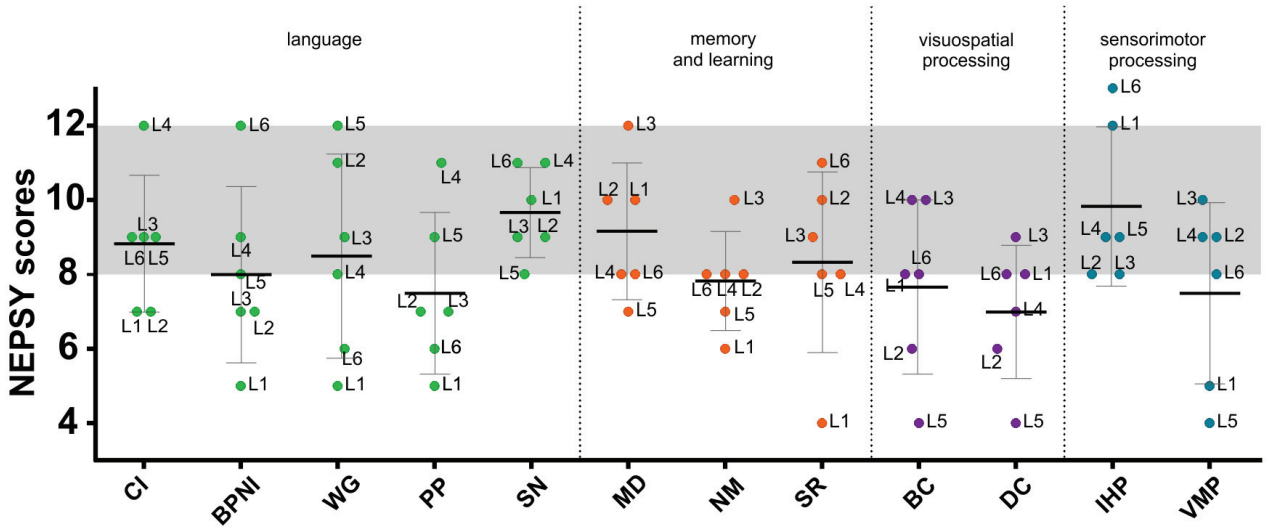

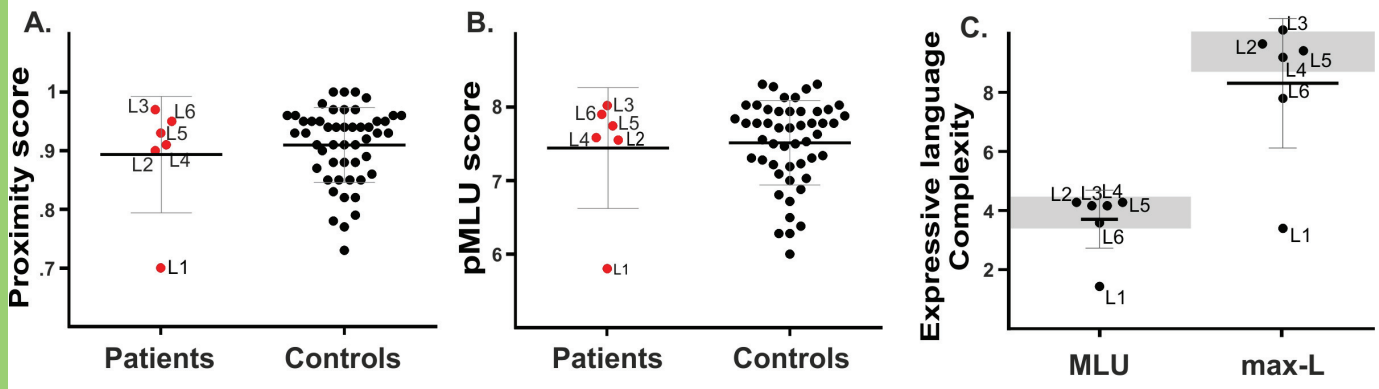

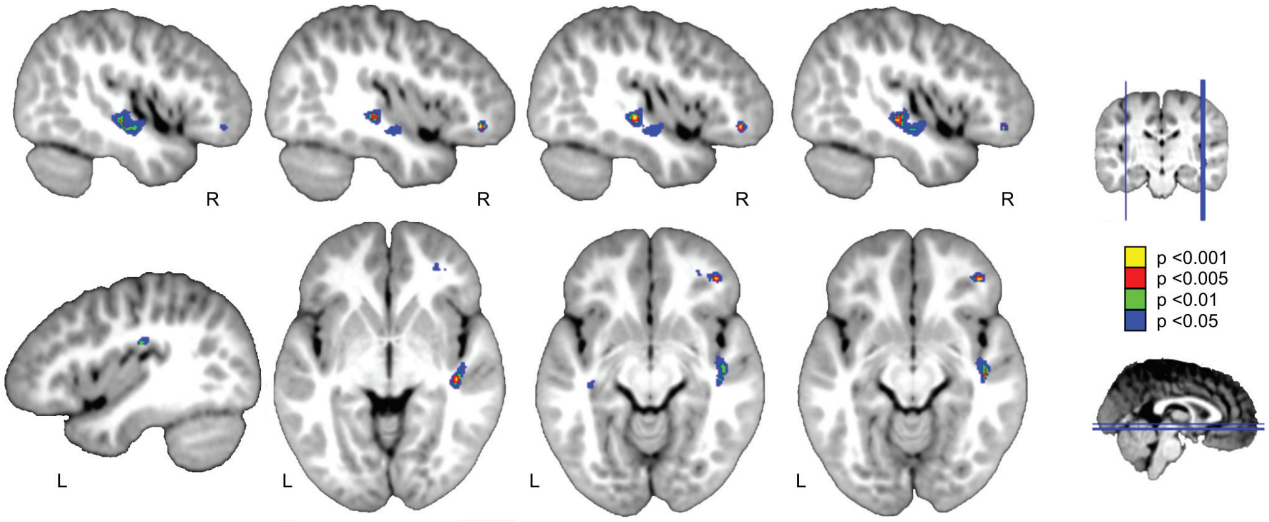

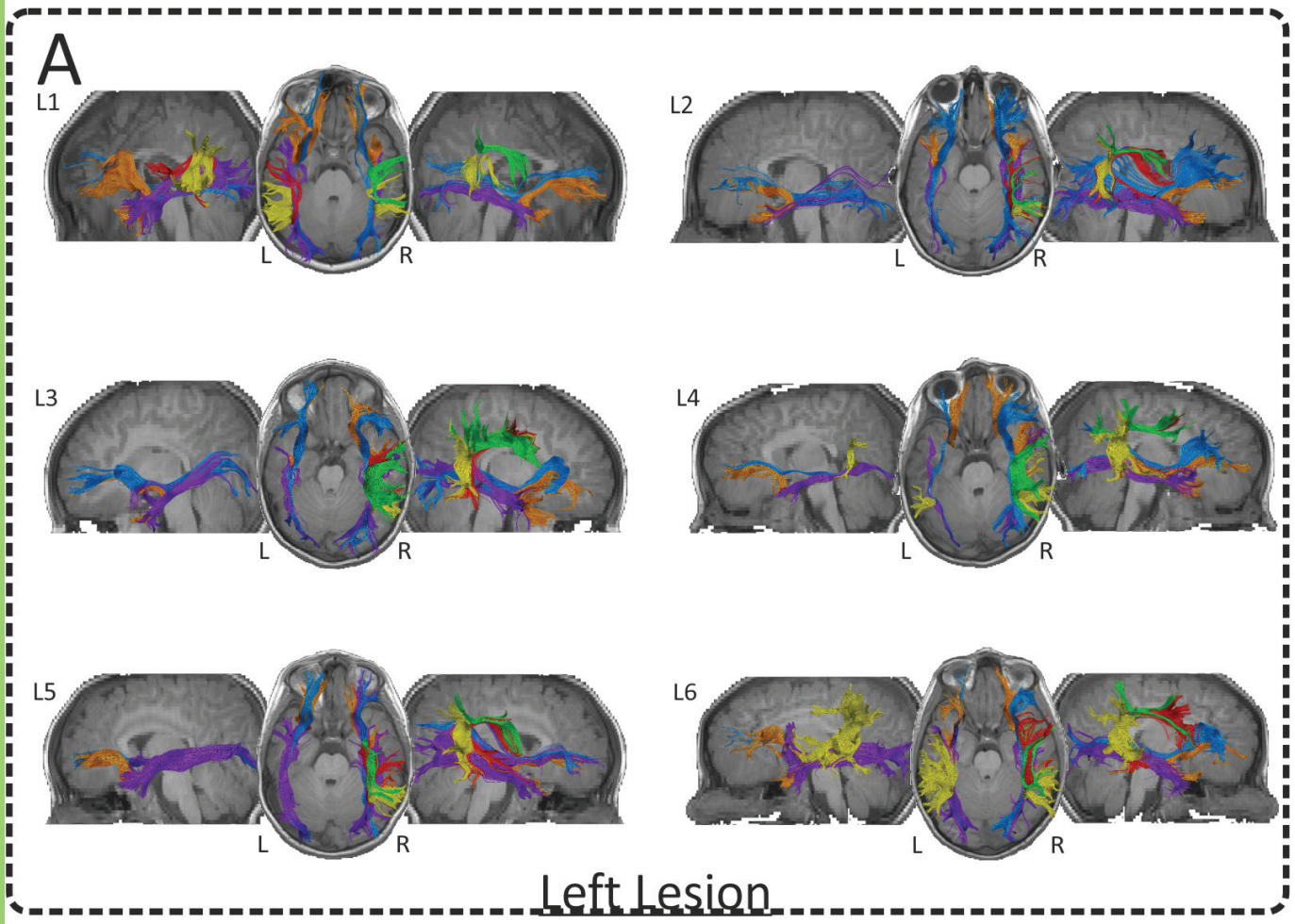

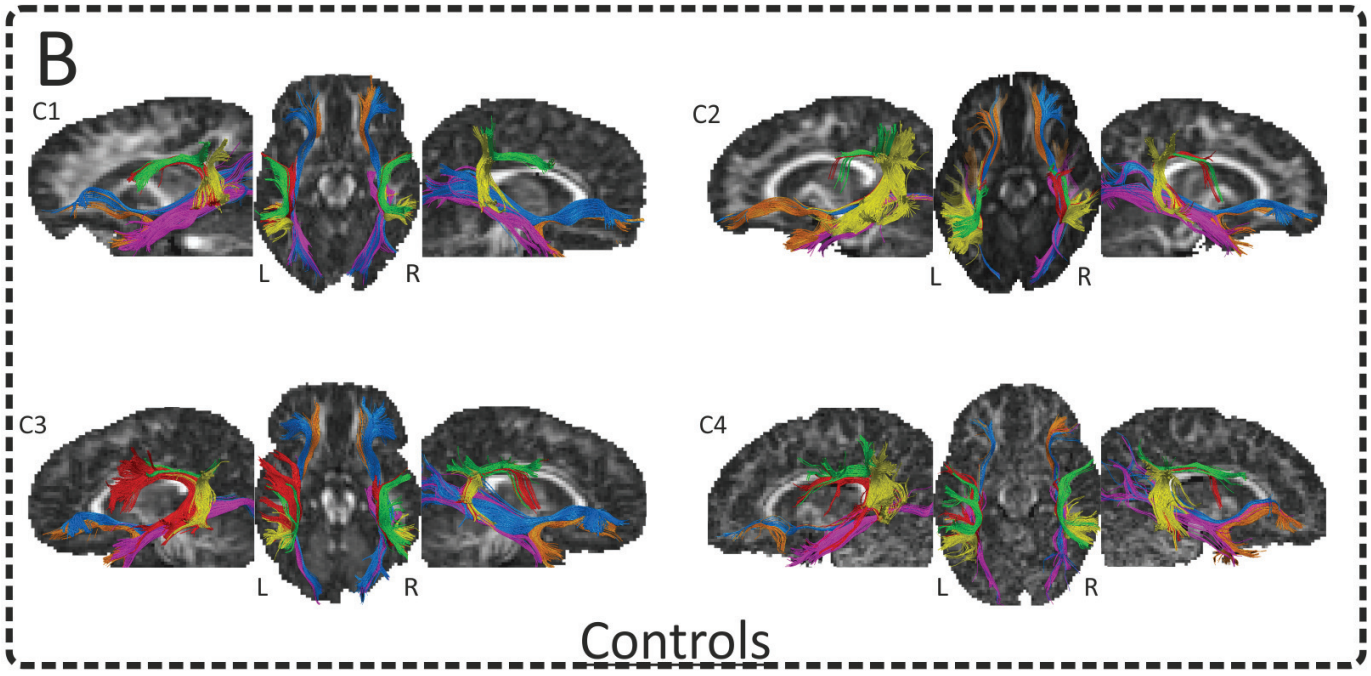

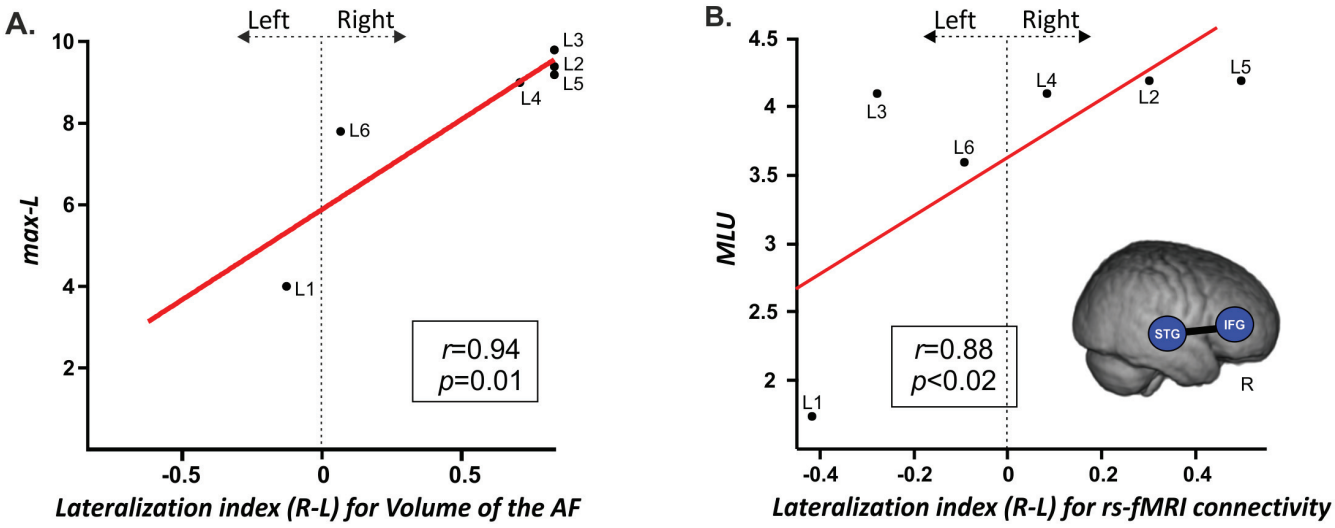

Table 1. Children demographic data and lesions main features.

Patient code	*Age at scan (years)*	*Gender*	*Gestational age at birth (weeks)*	*Birth weight (g)*	*Clinical debut (hours of age)*	*Age of MRI diagnostic (days)*	*Vascular territory*	Stroke Volume at birth *(mL)*	*Motor impairment (Hemiplegia)*	*Epilepsy**
L1	4	M	41	3160	Clonic Seizures at 12 hours	4 days	M2 L	18890	No	No
L2	3.5	F	41	2960	Clonic Seizures at 26 hours	10 days	M4 L	47428	Si	No
L3	4	M	40	3560	Clonic Seizures at 48 hours	20 days	M1 Post-bifurcation L	17588	No	No
L4	4	F	41	2600	Clonic Seizures at 18 hours	4 days	M2 sup L	27882	No	No
L5	4	M	39	3340	Clonic Seizures at 24 hours	5 days	M1 Post-bifurcation L	36512	No	No
L6	3.5	M	40	3025	Clonic Seizures at 41 hours	5 days	M1 Post-bifurcation L	23509	Si	No

* Epilepsy = at least two recurrent and unprovoked seizures.

Table 2. Phonological complexity and proximity scores for the children with PAIS (single values) and for the control group (means and standard deviations). The * indicates scores significantly different from the control group ($p < .05$) resulted from the modified *t*-test.

	Phon. complexity	Phon. proximity
L1	**5.81***	**0.70***
L2	7.56	0.90
L3	8.03	0.97
L4	7.59	0.91
L5	7.75	0.93
L6	7.91	0.95
Controls	7.44 (0.81)	0.89 (0.09)

Table 3. Spontaneous utterance performance (MLU and L-max scores) for the children with PAIS and for the control group (means and standard deviations).The * indicates scores significantly different from the control group ($p < .05$) resulted from the modified *t*-test.

	MLU	L-max
L1	**1.74***	**4***
L2	4.2	9.4
L3	4.1	9.8
L4	4.1	9
L5	4.2	9.2
L6	3.6	7.8
Controls	3.66 (0.96)	8.2 (2.16)

Table 4. Precise lesion location for each child with PAIS with the corresponding percentage over the total of the individual lesion size. The percentage of white matter and grey matter loss is also presented for each patient. IFG: Inferior frontal gyrus; MFG: Middle frontal gyrus; SMG: Supramarginal gyrus; AG: Angular gyrus; STG: Superior temporal gyrus; MTG: Middle temporal gyrus; MOG: Middle occipital gyrus

Patient code	*Lesion location*	*% of GM loss*		*% of WM loss*	
		Left	*Right*	*Left*	*Right*
L1	L Precentral gyrus (39%) L IFG (19%) L Postcentral gyrus (16%) L MFG (16%)	0.37	.	2.5	.
L2	L SMG (56%) L AG (33%) L STG (10%)	4.4	.	7.7	.
L3	L AG (40%) L MOG (25%) L SMG (12%)	7.8	.	10.3	.
L4	L Postcentral gyrus (53%) L SMG (23%) L Precentral gyrus (20%)	4.3	.	0.8	.
L5	L AG (28%) L STG (26%) L SMG (19%) L MTG (8%)	12.1	.	7.4	.
L6	L IFG (39%) L MFG (33%) L Precentral gyrus (24%)	0.6	.	1.7	.